Interspecies quorum sensing in co-infections can manipulate trypanosome transmission potential

Interspecies quorum-sensing in co-infections can manipulate trypanosome transmission potential

Eleanor Silvester, Julie Young, Alasdair Ivens, and Keith R. Matthews*

Centre for Immunity, Infection and Evolution; Institute for Immunology and Infection Research, School of Biological Sciences, University of Edinburgh.

*Corresponding author:
Keith R. Matthews,
Email keith.matthews@ed.ac.uk

Quorum sensing (QS) is commonly used in microbial communities and some unicellular parasites to coordinate group behaviours[1,2]. An example is *Trypanosoma brucei* that causes Human African trypanosomiasis, as well as the livestock disease, nagana. Trypanosomes are spread by tsetse flies, transmission being enabled by cell-cycle arrested 'stumpy forms' that are generated in a density-dependent manner in mammalian blood. QS is mediated through a small (<500 Da), non-proteinaceous, stable but unidentified 'stumpy induction factor'[3], whose signal response pathway has been identified. Although QS is characterised in *T. brucei*, co-infections with other trypanosome species (*T. congolense, T. vivax*) are common in animals, generating the potential for interspecies interactions. Here, we show that *T. congolense* exhibits density-dependent growth control *in vivo* and conserves QS-regulatory genes, of which one can complement a *T. brucei* QS signal-blind mutant to restore stumpy formation. Thereafter we demonstrate that *T. congolense*-conditioned culture medium promotes *T. brucei* stumpy formation *in vitro*, dependent upon integrity of the QS signalling pathway. Finally, we show that, *in vivo*, co-infection with *T. congolense* accelerates differentiation to stumpy forms in *T. brucei*, this also being QS dependent. These cross-species interactions have important implications for trypanosome virulence, transmission, competition and evolution in the field.

Trypanosoma brucei, Trypanosoma congolense and *Trypanosoma vivax* are African trypanosome species that can infect game animals and livestock, with a co-infection frequency of up to 25% where analysed[4-7]. All three species are spread by tsetse flies but undergo distinctive developmental paths within the arthropod vector[8]. Furthermore, only *Trypanosoma brucei* is reported to undergo developmental transformation in the bloodstream of mammalian hosts in preparation for transmission, generating 'stumpy forms' that are G1 arrested and morphologically distinct from 'slender forms' that proliferate to establish each wave of parasitaemia[9].

Other trypanosome species are described as monomorphic, or have ill-defined morphological heterogeneity in the historical literature[10-12], although *T. vivax* can accumulate in a G1 arrested form[13]. To determine whether *T. congolense* exhibits density dependent cell-cycle arrest in the mammalian bloodstream, six mice infected with *T. congolense* ILTat3000 were monitored for their kinetoplast (K) and nuclear (N) configuration[14], a cytological indicator of cell cycle position. Analysis over the first 14 days of infection demonstrated that parasite number had a significant negative effect on the proportion of proliferating (2K1N, 2K2N) cells (general linear model, p=0.001) (Figure 1a) such that parasites accumulated with a 1K1N configuration in individual infections when their numbers exceeded approximately $8x10^7$/ml (Supplementary Figure 1). Although this was not associated with an accompanying morphological transition equivalent to *T. brucei* stumpy formation (Figure 1b-d), BLAST and reciprocal BLAST analysis of the genome of *T. congolense* identified potential orthologues of a characterised set of 25 *T. brucei* genes required for stumpy formation[15] (Supplementary Table 1), there being a similar number in the *T. vivax* genome. Hence *T. congolense* demonstrated density-dependent cell-cycle arrest *in vivo* and encodes predicted orthologues of components of the *T. brucei* stumpy formation pathway.

To explore conservation of the signalling pathway responsible for stumpy formation between *T. congolense* and *T. brucei*, functional complementarity was examined (Figure 2). Null mutants for *Tb*927.9.4080 ('*Tb*HYP2', previously identified as a component of the *T. brucei* QS response pathway[15]; Supplementary table 2 and Supplementary Figure 2) were initially generated in pleomorphic *T. brucei* EATRO 1125 by sequential allelic replacement (*T. brucei* AnTat1.1 90:13 Δ*Tb*HYP2; Supplementary Figure 3). As expected for a QS signalling pathway component, *Tb*HYP2 null mutants lost the capacity for growth control *in vivo* (Supplementary Figure 4). They also did not express the PAD1 marker for stumpy forms[16] (Supplementary Figure 4) and, when harvested and exposed to the developmental trigger cis-aconitate, differentiated to the next life-cycle stage (procyclic forms) less efficiently than wild type parasites as assessed by expression of the procyclic

surface protein EP procyclin and proliferation (Supplementary Figure 4). Thereafter, the *Tb*HYP2 null mutants were engineered (Figure 2a) for doxycycline-inducible ectopic expression of the *T. congolense* orthologue of *Tb*HYP2 (*Tc*IL3000.0.19510, '*Tc*HYP2'; E value: 5.9e-262, 45% identity, 58% similarity to *Tb*HYP2; Supplementary Table 1). Figure 2b shows that upon inducible expression of *Tc*HYP2, there was slowed progression of the parasitaemia *in vivo*, potentially linked to either a premature development to stumpy forms caused by overexpression of the QS-signal pathway orthologue or a dominant negative consequence of *Tc*HYP2 expression. Supporting the former, those parasites induced to express *Tc*HYP2 exhibited PAD1 expression, whilst uninduced parasites remained PAD1 negative (Figure 2c). Further, when exposed to cis-aconitate the induced parasites expressed EP procyclin more effectively than the uninduced lines after 4h and 24h (Figure 2d; $p<0.0001$ and $p=0.0082$ respectively). Combined these assays demonstrated that *Tc*HYP2 can restore stumpy formation in a *T. brucei* *Tb*HYP2 null mutant, demonstrating functional complementarity between the genes.

Next, to explore interspecies cross talk in QS signals, the capacity for *T. congolense* to release a signal capable of inducing stumpy formation in *T. br*ucei was tested. Initially, pleomorphic *T. brucei* (EATRO 1125 AnTat1.1 90:13; capable of stumpy formation), monomorphic *T. brucei* (Lister 427 cells; incapable of stumpy formation) or culture-adapted *T. congolense* cells (ILTat3000) were incubated in the presence of 50% or 75% conditioned medium from *T. congolense* culture (harvested from a *T. congolense* culture that had proliferated to $6x10^6$/ml after 3 days without passage). These parasite species grow optimally in different culture media but *T. brucei* can grow effectively in *Tc*N medium (75% *Tc*BSF3 *T. congolense* growth medium[17] plus 25% HMI-9 *T. brucei* culture medium[18]). Supplementary Figure 5a demonstrates that *T. congolense* grew uninterrupted in the presence of its own conditioned medium ('*Tc*CM'), demonstrating it could still support active proliferation uninhibited by the accumulation of toxic metabolites. In contrast, *T. brucei* showed reduced growth with *Tc*CM, this being more pronounced with the pleomorphic line than the monomorphic line (Supplementary Figure

5b, 5c). To assess whether this reflected a progression to stumpy formation in pleomorphic cells, a reporter line was exploited with the chloramphenicol acetyl transferase (CAT) gene expressed under the control of the PAD1 3'UTR that governs its stumpy-specific gene expression[19]. In this case, *Tc*CM reduced growth (Figure 3a) and generated a 2.1fold (p=0.0002) increase in activation of the CAT reporter after 2 days compared to *Tc*N, equivalent to the activation generated by *T. brucei* AnTat1.1 90:13 conditioned medium (*Tb*CM; 1.9-fold, p=0.0006) (Figure 3b). To explore whether the CAT-reporter response was mediated via the QS-signalling pathway, the same analysis was carried out using a cell line containing the CAT-PAD 3'UTR reporter construct but which was also capable of inducible RNAi of *Tb*HYP2 (*T. brucei* AnTat1.1 90:13 CAT-PAD *Tb*HYP2 RNAi). When exposed to conditioned medium from *T. brucei* (*Tb*CM, Figure 3c) or *T. congolense* (*Tc*CM, Figure 3d) for 48h and 72h, CAT reporter expression was significantly reduced upon *Tb*HYP2 RNAi compared to cells where *Tb*HYP2 RNAi was not induced (*Tc*CM at 48h, p=0.0009; *Tb*CM at 48h, p<0.0001). Cell cycle arrest in response to *Tb*CM and *Tc*CM was also reduced upon *Tb*HYP2 RNAi (Supplementary Figure 6). Confirming this was mediated through a QS response, a CAT reporter controlled by the 3'UTR of the constitutively-expressed *T. brucei* aldolase gene was not significantly affected by *Tb*HYP2 RNAi when exposed to *Tb*CM or a cell permeable mimic of the QS signal, 8-pCPT-cAMP[20] (Supplementary Figure 7). Hence, *T. congolense* conditioned medium, as well as *T. brucei* conditioned medium, can promote growth arrest and activation of stumpy reporter gene expression in pleomorphic *T. brucei in vitro*, this being mediated through the QS signalling pathway. In contrast, culture-adapted *T. congolense* did not show growth inhibition in *T. brucei* conditioned medium containing QS-signal activity sufficient to arrest *T. brucei* (Supplementary Figure 5d, 5e). It remains to be established whether *T. congolense* are not responsive to the *T. brucei* QS-signal or if this is a consequence of the culture-adapted *T. congolense* line used in the *in vitro* experiments, which have been subject to long term passage. Unlike *T. brucei* conditioned medium, 8-pCPT-cAMP could inhibit *T. congolense* growth *in vitro*, supporting the conservation of a QS signalling pathway between the

species, although the effect was less pronounced than with *T. brucei* (Supplementary Figure 5f, 5g).

Having demonstrated the potential for cross-talk in QS signals between *T. congolense* and *T. brucei in vitro*, we examined whether the same response was detectable in co-infections between these species *in vivo*. To enable unambiguous identification of *T. brucei* in the mixed infection, we generated a *T. brucei* pleomorphic line encoding a Ty1 epitope tagged PFRA protein (*T. brucei* AnTat1.1 90:13 PFR-Ty1)[21]. This allowed flagellar staining to distinguish *T. brucei* from *T. congolense*, with simultaneous co-labelling with PAD1 antibody and morphological analysis permitting quantitation of stumpy formation (Figure 4a). Infections were initiated with *T. congolense* followed, on day 4 post-infection, with a super-infection with *T. brucei* (Supplementary Figure 8a). Control infections involving either *T. congolense* or *T. brucei* alone were analysed in parallel. The contribution of each species to the overall parasite load was then determined by scoring cell number and PFR labelling (Figure 4b), as was *T. brucei* PAD1 expression (Figure 4c) and cell-cycle status (Supplementary Figure 9). In the presence of a co-infection with *T. congolense, T. brucei* generated more PAD1-positive cells at a lower overall density of *T. brucei* than in *T. brucei* infections alone (Figure 4c). Thus, 50% of *T. brucei* cells were PAD1-positive in the co-infection compared with <10% in the mono-infection ($p=0.0044$), despite the *T. brucei* parasites comprising only a small proportion of the total parasite load, which was similar in the single species and mixed species infections ($1x10^8$ cells/ml; Supplementary Figure 8a). Furthermore, although comprising only a minority of the overall parasitaemia in the co-infection (Figure 4b), the *T. brucei* parasites had assumed a stumpy morphology and exhibited an accumulation of cells with a 1 kinetoplast, 1 nucleus configuration ($p=0.015$; Supplementary Figure 9). To confirm that *T. brucei* stumpy formation was mediated via the QS-signalling pathway, co-infection was repeated using a PFR-epitope tagged *T. brucei* line capable of RNAi-mediated silencing of *Tb*HYP2 under doxycycline regulation *(T. brucei* AnTat1.1 90:13 PFR-Ty1 *Tb*HYP2 RNAi). Effective *Tb*HYP2 silencing in this cell line was confirmed at the RNA level (Figure 4d), this being expected to inhibit differentiation to stumpy forms *in*

vivo. When co-infected with *T. congolense* (Supplementary Figure 8b, Figure 4e), in the absence of *Tb*HYP2 silencing, *T. brucei* stumpy formation was accelerated (Figure 4f) confirming the outcome with *T. brucei* AnTat1.1 90:13 PFR-Ty1 cells (Figure 4c). However, with *Tb*HYP2 silencing, the prevalence of PAD1-positive *T. brucei* cells was significantly less ($p<0.0001$) (Figure 4f, Supplementary Figure 10) as was the accumulation of cells with 1K1N ($p=0.007$; Supplementary Figure 11), despite equivalent numbers of *T. brucei* in each infection. Hence, co-infection with *T. congolense* induces *T. brucei* to generate stumpy forms at low relative parasitaemia, with dependence upon integrity of the *T. brucei* QS signalling pathway demonstrating that this is mediated through QS cross-talk between the species *in vivo*.

In combination, our results have established, firstly, that *T. congolense* is capable of density sensing *in vivo*, generating cell-cycle arrested forms akin to the stumpy forms of *T. brucei*, albeit without significant morphological transformation. Secondly, and consistent with this, the genome of the parasite encodes many molecules with similarity to components previously implicated in *T. brucei* QS responses, at least one of which can functionally complement a *T. brucei* null mutant to rescue stumpy formation. Moreover, 8-pCPT-cAMP which mimics the QS signal in *T. brucei*, also promotes growth inhibition in *T. congolense* supporting conservation of the signalling pathway. Finally, we have demonstrated that *T. congolense* can generate a QS signal that drives *T. brucei* stumpy formation *in vitro* and during co-infections, and that this effect is lost when the *T. brucei* QS signalling pathway is silenced, demonstrating transduction via the same molecular pathway as the *T. brucei* QS signal. This demonstrates the capacity for inter-species QS between *Trypanosoma congolense* and *Trypanosoma brucei* in simultaneously infected hosts. Interestingly, our results provide clear evidence of *T. congolense* signalling to *T. brucei* but the converse was less obvious. Whether this indicates that signalling is unidirectional or whether our culture adapted *T. congolense* line are less sensitive to the QS signal remains to be established.

Trypanosome infections are sustained long-term in mammalian hosts in the field, such that the capacity for interaction within and between species

in co-infections has the potential to generate distinct evolutionary responses[22,23]. For example, the production of a co-received QS signal may favour a pre-existing parasite population by preventing a secondary incoming trypanosome species proliferating and so establishing, a feature described in malaria infections[24,25]. Reduced sensitivity to the shared QS signal may also be selected in the context of an established co-infection to improve competitive fitness. Finally, if production of the QS signal was resource costly, cheats that produce less signal could exploit that of the co-infecting parasites to assist their transmissibility[26,27]. These scenarios may each select parasites whose capacity for virulence and transmissibility is adapted to the presence of a competing species. However, if transferred to naive hosts without competitors, parasites adapted for co-infection might exhibit a different infection dynamic, potentially exhibiting enhanced virulence through their reduced sensitivity to QS signals. As well as *T. brucei brucei*, that can only infect animals, livestock and game animals are the long-term reservoir of human infective *Trypanosoma brucei rhodesiense*[28] and, potentially, *Trypanosoma brucei gambiense*. Where human infective *T. brucei* coexist with *T. congolense*, the transition from long-term maintenance in a co-infected game reservoir into a monospecies infection in a human host may contribute, with host factors and other parasite factors, to the variability in parasite burden generated by different parasite isolates[29,30].

References

1. Brown, S.P. and A. Buckling.A social life for discerning microbes, *Cell*, 2008. **135**(4): p. 600-3.
2. Leggett, H.C., S.P. Brown, and S.E. Reece.War and peace: social interactions in infections, *Philos Trans R Soc Lond B Biol Sci*, 2014. **369**(1642): p. 20130365.
3. Vassella, E., B. Reuner, B. Yutzy, and M. Boshart.Differentiation of African trypanosomes is controlled by a density sensing mechanism which signals cell cycle arrest via the cAMP pathway, *Journal of Cell Science*, 1997. **110**: p. 2661-2671.
4. Auty, H., N.E. Anderson, K. Picozzi, T. Lembo, J. Mubanga, R. Hoare, R.D. Fyumagwa, B. Mable, L. Hamill, S. Cleaveland, *et al.*Trypanosome diversity in wildlife species from the serengeti and Luangwa Valley ecosystems, *PLoS Negl Trop Dis*, 2012. **6**(10): p. e1828.
5. Cox, A.P., O. Tosas, A. Tilley, K. Picozzi, P. Coleman, G. Hide, and S.C. Welburn.Constraints to estimating the prevalence of trypanosome infections in East African zebu cattle, *Parasit Vectors*, 2010. **3**: p. 82.
6. Takeet, M.I., B.O. Fagbemi, M. De Donato, A. Yakubu, H.E. Rodulfo, S.O. Peters, M. Wheto, and I.G. Imumorin.Molecular survey of pathogenic trypanosomes in naturally infected Nigerian cattle, *Res Vet Sci*, 2013. **94**(3): p. 555-61.
7. Pinchbeck, G.L., L.J. Morrison, A. Tait, J. Langford, L. Meehan, S. Jallow, J. Jallow, A. Jallow, and R.M. Christley.Trypanosomosis in The Gambia: prevalence in working horses and donkeys detected by whole genome amplification and PCR, and evidence for interactions between trypanosome species, *BMC Vet Res*, 2008. **4**: p. 7.
8. Rotureau B and J. Van Den Abbeele.Through the dark continent: African trypanosome development in the tsetse fly., *Front Cell Infect Microbiol.*, 2013. **3**(53).
9. Vickerman, K.Polymorphism and mitochondrial activity in sleeping sickness trypanosomes, *Nature*, 1965. **208**(12): p. 762-6.
10. Vickerman, K.The fine structure of Trypanosoma congolense in its bloodstream phase, *J Protozool*, 1969. **16**(1): p. 54-69.
11. Gardiner, P.R. and A.J. Wilson.Trypanosoma (Duttonefla) vivax, *Parasitol Today*, 1987. **3**(2): p. 49-52.
12. Nantulya, V.M., J.J. Doyle, and L. Jenni.Studies on Trypanosoma (nannomonas) congolense. I. On the morphological appearance of the parasite in the mouse, *Acta Trop*, 1978. **35**(4): p. 329-37.
13. Shapiro, S.Z., J. Naessens, B. Liesegang, S.K. Moloo, and J. Magondu.Analysis by flow cytometry of DNA synthesis during the life cycle of African trypanosomes, *Acta Trop*, 1984. **41**(4): p. 313-23.
14. Sherwin, T. and K. Gull.The cell division cycle of Trypanosoma brucei brucei: timing of event markers and cytoskeletal modulations, *Philos Trans R Soc Lond B Biol Sci*, 1989. **323**(1218): p. 573-88.
15. Mony, B.M., P. MacGregor, A. Ivens, F. Rojas, A. Cowton, J. Young, D.

Horn, and K. Matthews.Genome-wide dissection of the quorum sensing signalling pathway in Trypanosoma brucei, *Nature*, 2014. **505**(7485): p. 681-5.
16. Dean, S.D., R. Marchetti, K. Kirk, and K. Matthews.A surface transporter family conveys the trypanosome differentiation signal, *Nature* 2009. **459**: p. 213-217.
17. Coustou, V., F. Guegan, N. Plazolles, and T. Baltz.Complete in vitro life cycle of Trypanosoma congolense: development of genetic tools, *PLoS Negl Trop Dis*, 2010. **4**(3): p. e618.
18. Hirumi, H. and K. Hirumi.Continuous cultivation of Trypanosoma brucei blood stream forms in a medium containing a low concentration of serum protein without feeder cell layers, *J Parasitol*, 1989. **75**(6): p. 985-9.
19. MacGregor, P. and K.R. Matthews.Identification of the regulatory elements controlling the transmission stage-specific gene expression of PAD1 in Trypanosoma brucei, *Nucleic Acids Res*, 2012. **40**(16): p. 7705-17.
20. Laxman, S., A. Riechers, M. Sadilek, F. Schwede, and J.A. Beavo.Hydrolysis products of cAMP analogs cause transformation of Trypanosoma brucei from slender to stumpy-like forms, *Proc Natl Acad Sci U S A*, 2006. **103**(50): p. 19194-9.
21. Bastin, P., Z. Bagherzadeh, K.R. Matthews, and K. Gull.A novel epitope tag system to study protein targeting and organelle biogenesis in Trypanosoma brucei, *Mol Biochem Parasitol*, 1996. **77**(2): p. 235-9.
22. Eswarappa, S.M., S. Estrela, and S.P. Brown.Within-host dynamics of multi-species infections: facilitation, competition and virulence, *PLoS One*, 2012. **7**(6): p. e38730.
23. Balmer, O., S.C. Stearns, A. Schotzau, and R. Brun.Intraspecific competition between co-infecting parasite strains enhances host survival in African trypanosomes, *Ecology*, 2009. **90**(12): p. 3367-78.
24. Bruce, M.C., C.A. Donnelly, M.P. Alpers, M.R. Galinski, J.W. Barnwell, D. Walliker, and K.P. Day.Cross-species interactions between malaria parasites in humans, *Science*, 2000. **287**(5454): p. 845-8.
25. Portugal, S., C. Carret, M. Recker, A.E. Armitage, L.A. Goncalves, S. Epiphanio, D. Sullivan, C. Roy, C.I. Newbold, H. Drakesmith, *et al.*Host-mediated regulation of superinfection in malaria, *Nat Med*, 2011. **17**(6): p. 732-7.
26. MacGregor, P., B. Szoor, N.J. Savill, and K.R. Matthews.Trypanosomal immune evasion, chronicity and transmission: an elegant balancing act, *Nat Rev Microbiol*, 2012. **10**(6): p. 431-8.
27. Diggle, S.P., A.S. Griffin, G.S. Campbell, and S.A. West.Cooperation and conflict in quorum-sensing bacterial populations, *Nature*, 2007. **450**(7168): p. 411-4.
28. Fevre, E.M., B.V. Wissmann, S.C. Welburn, and P. Lutumba.The burden of human African trypanosomiasis, *PLoS Negl Trop Dis*, 2008. **2**(12): p. e333.
29. MacLean, L., J.E. Chisi, M. Odiit, W.C. Gibson, V. Ferris, K. Picozzi, and J.M. Sternberg.Severity of human african trypanosomiasis in East

Africa is associated with geographic location, parasite genotype, and host inflammatory cytokine response profile, *Infect Immun*, 2004. **72**(12): p. 7040-4.
30. MacLean, L.M., M. Odiit, J.E. Chisi, P.G. Kennedy, and J.M. Sternberg.Focus-specific clinical profiles in human African Trypanosomiasis caused by Trypanosoma brucei rhodesiense, *PLoS Negl Trop Dis*, 2010. **4**(12): p. e906.

End Notes

Supplementary Information is linked to the online version of the paper at www.nature.com/naturemicrobiology

Correspondence and requests for materials should be addressed to Keith Matthews (keith.matthews@ed.ac.uk)

Acknowledgements

This work was supported by a Wellcome Trust Investigator award (103740/Z/14/Z) and Royal Society Wolfson Research merit award (WM140045) to KM and a BBSRC studentship to ES. The Centre for Immunity, Infection and Evolution is supported by a Strategic Award from the Wellcome Trust (095831). We thank Margo Chase-Topping for assistance with statistical analysis, Martin Waterfall for assistance with flow cytometry and Jacqueline Matthews for comments on the manuscript.

Author Contributions

Conceived and supervised the study (KRM), devised the experiments (ES, KRM), planned and carried out the experiments (ES, JY), collated, analysed and interpreted the data (ES, KRM, AI), wrote the manuscript (KRM, ES).

Competing financial interests

The authors declare that they have no competing financial interests in relation to this work.

Figure legends

Figure 1

T. congolense cell cycle analysis reveals a reduction in proliferating cells at the peak of parasitaemia.

a) Cell cycle analysis over the first 14 days of infection for six mice infected with *T. congolense* ILTat3000. The slope of the percentage of proliferating cells (2K1N – G2-phase cells, 2K2N – post-mitotic cells) and the parasitaemia showed significant deviation from zero (p=0.0003). 500 parasites were scored per sample unless parasitaemias were very low, when 200 cells were scored.
b) Phase contrast images of *T. brucei* slender (3 days post infection) and stumpy forms (6 days post infection) (top) and *T. congolense* ILTat3000 over 7 days of infection. Cells were counterstained with DAPI to reveal the nucleus and kinetoplast. Scale bar= 10µm.
c) Forward and side scatter profiles of slender (3 days post infection, n=2) and stumpy form (6 days post infection, n=2) parasites highlighting morphological differences between the developmental forms.
d) Forward and side scatter profiles of *T. congolense* ILTat3000 during ascending parasitaemia (5 days post infection, n=2) or at the first peak of parasitaemia (7 days post infection, n=2). Inset images show the absence of morphological difference between each population. Scale bar= 10µm.

Figure 2

*A T. congolense orthologue of a T. brucei QS response pathway component, Tb*HYP2*, can restore stumpy formation in a T. brucei Tb*HYP2 *null mutant in murine infections.*

a) A *T. brucei* EATRO 1125 *Tb*Hyp2 null mutant was generated by sequential allelic replacement in the parental cell line *T. brucei* AnTat1.1 90:13. The *Tb*Hyp2 null mutant (*T. brucei* AnTat1.1 90:13 *Tb*HYP2 dKO) was then transfected with a construct for the doxycycline-inducible ectopic expression of *Tc*HYP2 (*Tc*HYP2 OE in KO).
b) Growth of the *T. brucei* EATRO 1125 *Tb*Hyp2 null mutant cell line with doxycycline-inducible TcHYP2 expression (TcHyp2 OE in KO) in mice. Parasite population growth was limited in infections where *Tc*HYP2 ectopic expression was induced (+Dox, red lines, n=3) relative to uninduced controls (-Dox, blue lines, n=3). Parental *T. brucei* AnTat 1.1 90:13 (black line, n=1) and *T. brucei* EATRO 1125 *Tb*HYP2 null mutant (navy line, n=1) cell lines were included as controls (further replicates are provided in Supplementary Figure 4). Crosses indicate humane euthanasia when infections were anticipated to be lethal within 12 hours.
c) Expression of the stumpy marker PAD1 was higher when *Tc*HYP2 was ectopically expressed in the *T. brucei* EATRO 1125 *Tb*Hyp2 null mutant than in the uninduced control. TY1-tagged *Tc*HYP2 protein was detected with BB2 antibody in +Dox samples but not in –Dox samples. Glucose-6-phosphate dehydrogenase, loading control.

d) Cells induced to express *Tc*HYP2 (+Dox, n=3) had increased capacity to differentiate to procyclic forms relative to uninduced cells (-Dox, n=3) following treatment with cis-aconitate, as determined by EP procyclin expression at 4h and 24h after treatment (unpaired t test, $p<0.0001$, $p<0.01$, two-sided). Bars represent mean ± SD). Parental *T. brucei* AnTat 1.1 90:13 stumpy (green, n=1) and culture-derived slender (orange, n=2) cells, as well as *T. brucei* EATRO 1125 *Tb*HYP2 null mutant (navy, n=1) cells were included as controls. Culture-derived procyclic cells (purple, n=1) were used as a positive control for procyclin expression.

Figure 3

Treatment with T. brucei- or T. congolense- conditioned medium inhibits growth of pleomorphic T. brucei via QS-signalling.

a) A pleomorphic *T. brucei* cell line (EATRO 1125) with a CAT reporter under the control of the PAD1 3'UTR (*T. brucei* AnTat1.1 90:13 CAT-PAD) was used to report on stumpy formation in response to conditioned medium treatment. Growth of this cell line was inhibited by treatment with 75% *T. brucei*- (*Tb*CM) or 75% *T. congolense*- (*Tc*CM) conditioned medium relative to non-conditioned control media (*Tb*N and *Tc*N). Data points represent the mean ± SEM of n=3 flasks.

b) CAT concentration/cell was elevated after 1 or 2 days of treatment with *Tb*CM or *Tc*CM (unpaired t test, $p<0.05$, $p<0.001$, two-sided). Bars represent mean ± SD of n=3 flasks. The effect of *Tc*CM was reproducible in three (out of three) independent experiments (one representative experiment is shown). The negative controls expressed an elevated CAT concentration/cell on day 3 because cultures were maintained without passage such that cell growth caused accumulation of the QS signal.

c) A CAT PAD 3'UTR reporter construct was transfected into a pleomorphic cell line (*T. brucei* EATRO 1125 AnTat1.1 90:13) with the capacity for doxycycline-inducible knock down of the QS-signalling component *Tb*HYP2 (*T. brucei* AnTat1.1 90:13 CAT-PAD *Tb*HYP2 RNAi). When this cell line was treated with *Tb*CM, the increase in CAT concentration/cell was muted in cells where *Tb*HYP2 RNAi had been induced relative to uninduced cells. Bars represent the mean ± SEM of n=3 flasks.

d) When the same cell line was treated with *Tc*CM, the increase in CAT concentration/cell was diminished in cells where *Tb*HYP2 RNAi had been induced relative to uninduced cells. Comparisons between categories were made using two-way ANOVA followed by Tukey's multiple comparison test ($p<0.05$, $p<0.01$, $p<0.001$, $p<0.0001$). Bars represent the mean ± SEM of n=3 flasks. The effect of *Tc*CM and *Tb*CM on this cell line was reproducible in two (out of two) independent experiments (one representative experiment is shown).

Figure 4

Pleomorphic T. brucei introduced into an established T. congolense infection differentiate prematurely to stumpy forms in an effect mediated by QS-signalling.

a) Pleomorphic *T. brucei* EATRO 1125 encoding Ty1 epitope-tagged PFRA (*T. brucei* AnTat1.1 90:13 PFR-Ty1) were used to identify *T. brucei in* mixed infections by flagellar staining (green). Note that *T. congolense* cells show non-specific intracellular staining with the BB2 antibody that detects the Ty1 epitope. A PAD1-positive *T. brucei* stumpy cell (arrowhead) is shown surrounded by *T. congolense* cells on day 8 of the co-infection experiment. PAD1-red. DAPI-purple. Scale bar, 10μm.
b) The proportion of each parasite species was determined by scoring >2000 cells in the co-infections as PFR-Ty1 positive or negative, and applied to the total parasitaemia to calculate the effective parasitaemia of each species in the co-infections on days 6, 7 and 8. The effective *T. brucei* parasitaemia in the co-infections (purple, n=3) remained lower than in the control '*T. brucei* only' infections (blue, n=3). Green; *T. congolense* in the co-infections (n=3). Red; '*T. congolense* only' infections (n=3).
c) PAD1-positive *T. brucei* on day 8 of the experiment (>500 cells scored, n=3 for each condition tested). Despite lower *T. brucei* parasitaemia in the superinfections there was a higher percentage of PAD1-positive cells compared with the single species *T. brucei* infections (unpaired t test, $p<0.01$, two-sided). Error bars represent mean ± SD.
d) A cell line with a Ty1 epitope tagged PFRA protein and the capacity for doxycycline-inducible *Tb*HYP2 RNAi was generated. Effective RNAi targeting *Tb*HYP2 was confirmed by Northern blot using RNA collected after 48 hours of culture ± doxycycline. Ethidium bromide stained rRNA acts a loading control.
e) The proportion of parasites of each species was calculated as in the panel b (n=3 for each condition tested). The effective *T. brucei* parasitaemia was lower in superinfections than in '*T. brucei* only' infections, whether or not *Tb*HYP2 RNAi was induced. The effective *T. brucei* parasitaemia was higher in co-infections where *Tb*Hyp2 RNAi was induced (+Dox) than those without induction (-Dox), though the difference was not significant.
f) PAD1-positive *T. brucei* on day 8 of the experiment (>500 cells scored, n=3 for each condition tested). There were significantly more PAD1-positive *T. brucei* cells in the co-infections where *Tb*Hyp2 RNAi was not induced (30-45%) than in co-infections where *Tb*HYP2 RNAi was induced (1-3%) ($p<0.0001$, One-way ANOVA with Tukey's multiple comparisons test). Error bars represent mean ± SD.

Methods

Animal experiments Animals were allocated at random into treatment groups from a group of female, age matched adult MF1 mice, at least 10 weeks old. No blinding was done.

T. congolense IL3000 infections

T. congolense parasites of the IL3000 strain were used both for infections and *in vitro* experiments. This strain was derived from the ILC-49 strain that was isolated from a cow in the Trans Mara, Kenya[31]. The *T. congolense* IL3000 parasites used for *in vivo* experiments were provided by Dr Annette MacLeod (University of Glasgow) in a blood straw. The *T. congolense* IL3000 parasites used for *in vitro* experiments were supplied as culture-adapted bloodstream forms by Dr Liam Morrison (Roslin Institute, Edinburgh), who had received them from Professor Théo Baltz (University of Bordeaux). Six female MF1 mice were inoculated intraperitoneally with *T. congolense* ILTat3000. Parasitaemia was monitored daily from day 3 post-infection. Parasitaemia was estimated from a wet blood smear using the Herbert and Lumsden rapid matching method[32]. Air-dried blood smears were fixed in ice-cold methanol and stored at -20°C prior to cell cycle analysis.

T. brucei null mutant infections

Three female cyclophosphamide-treated MF1 mice were inoculated intraperitoneally with the *Tb*Hyp2 null mutant cell line. In parallel two mice were inoculated with the parental AnTat1.1 90:13 cell line. Parasitaemia was monitored daily from day 3 post-infection. Parasitaemia was estimated from a wet blood smear using the Herbert and Lumsden rapid matching method[32]. Infections were monitored until parasites differentiated to stumpy forms or were terminated if the uncontrolled ascending parasitaemia was predicted to become lethal within the next 12 hours. At the end of the experiment parasites were purified from whole blood by passage through a DE52 column (Whatman® anion exchange cellulose, Z742600) at pH 7.8.

Infections to test functional complementation

Six female cyclophosphamide-treated MF1 mice were inoculated intraperitoneally with the *Tc*Hyp2 overexpression *Tb*Hyp2 null mutant cell line. One group (n=3) was provided with doxycycline (200μg/ml in 5% sucrose) in their drinking water from the time of inoculation to induce *Tc*Hyp2 overexpression. The other group (n=3) received 5% sucrose only. In parallel one mouse was infected with AnTat1.1 90:13 and one mouse with the *Tb*HYP2 null mutant. Parasitaemia was monitored daily from day 3 post-infection. Parasitaemia was estimated from a wet blood smear using the Herbert and Lumsden rapid matching method[32]. Infections were monitored until parasites differentiated to stumpy forms or were terminated if the uncontrolled ascending parasitaemia was predicted to become lethal within the next 12 hours. At the end of the experiment parasites were purified from

whole blood by passage through a DE52 column (Whatman® anion exchange cellulose, Z742600) at pH 7.8.

Cell cycle analysis

Methanol-fixed blood smears were rehydrated in PBS for 5 min. Slides were stained with 30μl of DAPI (10μg/ml in PBS) for 2 min in a humidity chamber and were then washed for 5 min in PBS. Slides were then mounted with 40μl Mowiol containing 2.5% DABCO (1, 4-diazabicyclo[2.2.2]octane). Nucleus and kinetoplast configurations were recorded by manual cell counting. 500 cells were counted per sample and per timepoint except where there was very low parasitaemia, where 200 cells were counted.

Generation of a *Tb*HYP2 null mutant with inducible *Tc*HYP2 overexpression

pEnT6B-Y and pEnT6P-Y vectors[33] were used to generate the *Tb*HYP2 null mutant by sequential allelic replacement. Primers were designed to amplify regions of the 5'UTR and 3'UTR of *Tb*HYP2 in order to replace the endogenous gene with a cassette containing either a puromycin or blasticidin resistance marker. Constructs were used to transfect the pleomorphic AnTat1.1 90:13 cell line, and successful generation of a null mutant was confirmed by Southern blotting.

Primers (F primer: GGGTTTACTAGTATGGCCTCAGAGTCAGCG, R primer: GGGTTTGGATCCCTACCCCCGTCCCTGTCC) were designed to amplify *Tc*Hyp2 (*Tc*IL3000.0.19510) with appropriate terminal restriction sites for insertion into the pDex577-Y vector for tetracycline-inducible overexpression with an N-terminal TY epitope tag[21]. The overexpression construct was used to transfect the *Tb*HYP2 null mutant and inducible overexpression was confirmed by Western blotting using an anti-TY antibody (BB2[21]).

Southern blotting

A gene probe was produced to detect the presence of the *Tb*HYP2 gene and a 5'UTR probe was designed to detect the correct integration of both constructs. PCR reactions with Q5 high fidelity DNA polymerase (NEB, M0491S) were used to generate material for the 5'UTR probe (F primer: ACTAGTACATGCTGGTCGTCAGTATT, R primer: GGATCCATCAGTGCACGTATTCTACCA) and gene probe (F primer: GGGTTTACTAGTATGGCATCGGAGGCAGCG, R primer: GGGTTTGGATCCTTATTCGCCCCTAACTGC). Purified DNA was then used to generate DIG-labelled probes with the DIG High Prime labelling and detection starter kit II (Roche, 11585614910). 1μg of genomic DNA extracted from parental AnTat1.1 90:13 cells, cells with suspected single allelic replacement of *Tb*Hyp2 and cells with suspected double allelic replacement of *Tb*Hyp2 was digested overnight at 37°C by PstI (Promega, R6111). Digested DNA was divided between two lanes (one for each probe) and resolved on an agarose gel for 3h at 100V. The gel was then soaked successively in depurination solution (0.25M HCl), denaturation solution (1.5M NaCl/0.5M NaOH) and neutralisation solution (1M Tris/1.5M NaCl/pH7.4) prior to transfer of the DNA to a nylon membrane overnight. The membrane was then UV cross-linked. Hybridisation was carried out overnight

at 42°C with the DIG-labelled DNA probe in DIG Easy Hyb Buffer (Roche, 11603558001). The membrane was washed twice for 5 min in 2xSSC/0.1%SDS at RT, and then twice for 15 min on 0.5xSSC/0.1%SDS at 68°C. The membrane was blocked for 1h with Maleic acid buffer containing 1% DIG block, before addition of 2μl anti-DIG (Roche, 11093274910) and incubation for 30 min. Final detection used the chemiluminescent substrate CDP-Star (Roche, 11685627001) diluted 1:100 in detection buffer (100mM Tris HCl 100mM NaCl pH9.5).

Western blotting

Protein samples were resolved on SDS-PAGE gels and blotted onto nitrocellulose membrane. Primary antibody dilutions were prepared in 5% milk and the membrane was incubated overnight. αBB2 antibody[21] was used at 1:20 to detect the TY-tagged *Tc*Hyp2, αPAD1 antibody[16] was used at 1:1000. αG6PDH (glucose-6-phosphate dehydrogenase, kind gift of Professor Paul Michels, University of Edinburgh) was used for loading controls at 1:10,000, and αEF1 (elongation factor 1-alpha, Merck Millipore 05-235) was used for loading controls at 1:7000. Secondary antibodies were diluted in 50% PBS and 50% Li-cor blocking buffer. Both anti-mouse (IRDye® 680 goat anti-mouse, Li-cor) and anti-rabbit (goat anti-rabbit IgG (H+L) Dylight 800, Thermoscientific) secondary antibodies were diluted 1:7500. Immunofluorescence was detected on the Li-cor Odyssey imaging system.

***In vitro* differentiation to procyclic forms**

Parasites were resuspended at $2x10^6$/ml in SDM79 medium (GIBCO by Life technologies) containing 6mM cis-aconitate (Sigma, A3412) and were incubated at 27°C. Samples were collected for flow cytometry at 0h, 4h and 24h.

Flow cytometry

$2\text{-}5x10^6$ cells were washed twice in PBS prior to fixing in 500μl 2% formaldehyde/0.05% glutaraldehyde >1h at 4°C. Cells were then washed 3x in PBS and resuspended in 2%BSA:PBS for 30 min. Cells were then resuspended in primary antibody diluted in 2%BSA:PBS (αPAD1 was diluted 1:200, αEP procyclin (Cedar Lane laboratories) was diluted 1:500) and were incubated overnight at 4°C. The cells were washed twice in PBS and were resuspended in secondary antibody diluted in 2%BSA:PBS (α-rabbit CY5 and α-mouse FITC were each diluted 1:1000). The cells were washed twice in PBS and were resuspended in 500μl PBS containing 0.02μg/ml DAPI. Samples were then processed on an LSRII flow cytometer (BD Biosciences). Positive controls and secondary antibody only controls were included. Analysis was performed using FlowJo software (Tree Star).

Conditioned medium generation

For generation of conditioned medium, cultures of *T. brucei* AnTat1.1 90:13 were established at $1x10^5$cells/ml in HMI-9[34] and were incubated for 2 days at 37°C (and 5%CO_2). Conditioned medium was harvested when cells had reached a density of $2\text{-}3x10^6$/ml, by pelleting the cells and passing the

supernatant through a 0.22μm filter. Filtered supernatant was stored at 4°C. Cultures of *T. congolense* for generating conditioned medium were in most cases established at $1x10^5$ cells/ml in *Tc*BSF3[17] and were incubated for 3 days at 34°C (and 5%CO_2). Conditioned medium was collected at a range of densities from $5x10^6$ cells/ml to $1x10^7$ cells/ml, and prepared as for *T. brucei* conditioned medium by filtering of conditioned supernatant through a 0.22μm filter. Conditioned medium was stored for a maximum of 5 days at 4°C before use. Alongside flasks for conditioned medium generation, flasks containing either HMI-9 or *Tc*BSF3 without parasites were prepared, and this control medium was treated in the same way as the conditioned medium and used as a negative control in all conditioned medium experiments.

CAT reporter experiments

A pleomorphic cell line with a CAT reporter under the control of the PAD1 3'UTR was used to report on stumpy formation[19]. Additionally, a pleomorphic cell line with inducible *Tb*HYP2 RNAi[15] was transfected with the CAT PAD1 3'UTR construct or a control construct with CAT reporter expression controlled by the 3'UTR of the constitutively expressed aldolase gene[19].

The CAT reporter *T. brucei* cells were washed once with HMI-9 and resuspended at a density of $2x10^5$ cells/ml in a mixture of 75% conditioned medium or control medium and 25% HMI-9. Cultures were incubated for 3 days at 37°C (and 5%CO_2) without passage. Each day cell number was estimated using a Beckman Coulter Z2 Coulter Particle count and size analyser (or haemocytometer if there were a number of dead cells), and CAT ELISA samples were collected. For experiments involving Hyp2 RNAi, induction of the RNAi with doxycycline was initiated one day before the addition of conditioned medium, and was maintained throughout the experiment. CAT ELISA samples were prepared by collecting 5ml of culture, washing cells 3x with PBS, and resuspending in 1ml CAT lysis buffer (Roche) for 25 min at RT. The lysis reaction was centrifuged to pellet debris and the supernatant was snap frozen in liquid nitrogen and stored at -80°C.

Samples were analysed by CAT ELISA (Roche, 11363727001) to determine their CAT concentration according to the manufacturer's instructions. Each sample was loaded into two wells of a 96 well plate. The CAT concentration of the samples was estimated by comparing the absorbance at 405nm to that of a CAT standard curve (provided by the manufacturer). The standard curve included a range of CAT concentrations of 0.0625ng/ml CAT to 2ng/ml CAT, as well as a blank of 0ng/ml. Absorbance was measured using a BioTek ELx808 Absorbance Microplate reader with Gen5 data analysis software (BioTek). Reads of duplicate wells at 405nm were averaged and converted to CAT concentrations using the standard curve. CAT concentration/ cell was calculated using the number of cells in each 5ml sample collected during the experiment.

Superinfection experiment

Six female MF1 mice were inoculated intraperitoneally with *T. congolense* ILTat3000 on day 0, each mouse received approximately $2.4x10^6$ cells. On day 4, three *T. congolense*-infected and three previously uninfected mice were inoculated intraperitoneally with *T. brucei* AnTat1.1

90:13 with a TY-tagged PFR, each mouse received approximately $1.2x10^5$ cells. Stocks used for infection were mixed prior to division between mice to ensure that single species infections and co-infections were initiated with the same *T. brucei* inoculum.

Parasitaemia was monitored daily from day 4 post-infection. Total parasitaemia was estimated from a wet blood smear using the Herbert and Lumsden rapid matching method[32]. 10μl of blood was collected on each day of infection, and cells were washed in 200μl cold PSG and resuspended in 125μl cold PBS, and then 125μl 8% paraformaldehyde in PBS was added. Cells were fixed on ice for 10 min and then resuspended in 130μl 0.1M glycine in PBS, and kept at 4°C overnight. Samples were then resuspended in PBS and used for immunofluorescence. The proportion of the co-infection parasitaemia contributed by each species was estimated by counting the number of PFR-TY1 positive cells (>2000 cells scored). At the end of the experiment parasites were purified from whole blood by passage through a DE52 column (Whatman® anion exchange cellulose, Z742600) at pH 7.8. Purified parasites were paraformaldehyde fixed for immunofluorescence and these samples were used to determine the proportion of *T. brucei* that were PAD1 positive in the infections (>500 cells scored), as well as the KN configuration of these cells.

Superinfection experiment with *Tb*HYP2 RNAi induction

Six female MF1 mice were inoculated intraperitoneally with *T. congolense* ILTat3000 on day 0, each mouse received approximately $2.4x10^6$ cells. On day 4, all six *T. congolense*-infected and six previously uninfected mice were inoculated intraperitoneally with a *T. brucei* EATRO1125 AnTat1.1 90:13 cell line with a TY-tagged PFR and doxycycline-inducible RNAi targeting *Tb*HYP2, each mouse received approximately $1.2x10^5$ cells. Stocks used for infection were mixed prior to division between mice to ensure that all infections were initiated with the same *T. brucei* inoculum.

On day 1 of the experiment doxycycline (200μg/ml in 5% sucrose) was provided in the drinking water of three of the *T. congolense* infected mice and three of the uninfected mice, the remaining mice received 5% sucrose only. Parasitaemia was monitored and samples were collected as for the initial superinfection experiment.

Immunofluorescence

Paraformaldehyde fixed cells were adhered to Polysine® slides (VWR, 631-0107). 20μl 0.1% triton in PBS was applied to each well for 2 minutes, this was then aspirated and wells were washed with a large drop of PBS. Wells were blocked with 2% BSA:PBS for 45 minutes at 37°C in a humidity chamber, before application of 20μl primary antibody. Wells were incubated with primary antibody (diluted in 2% BSA:PBS, αPAD1 1:1000, BB2 1:20) for 45 minutes at 37°C in a humidity chamber. Positive control wells and secondary antibody only wells were included for each experiment. Wells were

each washed 5 times by repeatedly applying and aspirating 1x PBS. Wells were incubated with 20μl secondary antibody (diluted in 2% BSA:PBS, α-rabbit Alexa fluor 488 1:500, α-mouse Alexa fluor 568 1:500) for 45 minutes at 37°C in a humidity chamber. 20μl of a DAPI working dilution (10μg/ml in PBS) was then applied to each well for 1 minute, followed by 5 washes with PBS. Slides were mounted with a cover slip by application of Mowiol containing 2.5% DABCO. Slides were analysed on a Zeiss Axioskop 2 plus or Zeiss Axio Imager Z2, and QCapture software was used for image capture. Images of BB2, PAD1 and DAPI staining were overlaid in ImageJ 64[35] and cell counts were performed using the Cell Counter Plugin.

Bioinformatic analysis

The BLASTP tool on TritrypDB[36] was used for identification of orthologues.

Statistical analysis

Most statistical analyses were carried out in GraphPad Prism version 6 (GraphPad Software, La Jolla, California, USA, www.graphpad.com). A General Linear Model was used to analyse *T. congolense* parasitaemias for cell cycle arrest using Minitab®. This model tested the significance of the effect of parasitaemia on % 2K1N, 2K2N cells and incorporated mouse as a random factor, which was not significant ($p=0.55$) In all analyses a p-value <0.05 was considered significant. Where the analyses used work on the assumption of a normal distribution, the distribution of the data was assessed before performing the analyses, and if required the data was transformed prior to testing.

Animal studies and group sizes

Animal experiments were carried out according to the UK Animals (Scientific) Procedures act under a licence (PPL60/4373) issued by the UK Home Office and approved by the University of Edinburgh Local ethical committee.

For the analysis of phenotypes 3- 5 animals per treatment were routinely used for analysis. Our previous analyses (e.g. Mony, B.M., et al., Genome-wide dissection of the quorum sensing signalling pathway in Trypanosoma brucei. Nature, 2014. 505(7485): p. 681-5)[15] indicate that this sample size is sufficient to detect differences between cell lines and treatment groups (for example where gene silencing is activated by provision of doxycycline). Using that data as an exemplar, we tested 5 genes for effects with and without doxycycline mediated gene-silencing *in vivo*. Using cell cycle status as the measured parameter, the effect size ranged from 0.637 to 1.804. Those values were then used to calculate the power for different samples sizes. This showed that a sample size of 3-5 per group (+ or - DOX) , or total of 6 to 10 allowed us to achieve 80% power for all test genes except one. In our current manuscript, the visual analytical assays applied (manual scoring by microscope) to the different treatments and groups (cell cycle scoring, analysis of PAD1 staining, scoring of flagellar labelling for parasite species, morphological analysis) required analyses to be limited to 3 animals per

group. Data were examined before analysis to ensure normality and that no transformations were required. P values of less than 0.05 were considered statistically significant.

Data Availability

The datasets generated during and/or analysed during the current study are available either within the manuscript or from the corresponding author on reasonable request.

Methods References

31. Wellde, B., R. Lotzsch, G. Deindl, E. Sadun, J. Williams, and G. Warui.Trypanosoma congolense. I. Clinical observations of experimentally infected cattle, *Exp Parasitol*, 1974. **36**(1): p. 6-19.
32. Herbert, W.J. and W.H. Lumsden.*Trypanosoma brucei*: a rapid "matching" method for estimating the host's parasitemia, *Experimental Parasitology*, 1976. **40**(3): p. 427-31.
33. Kelly, S., J. Reed, S. Kramer, L. Ellis, H. Webb, J. Sunter, J. Salje, N. Marinsek, K. Gull, B. Wickstead, *et al.*Functional genomics in *Trypanosoma brucei*: A collection of vectors for the expression of tagged proteins from endogenous and ectopic gene loci, *Molecular and Biochemical Parasitology*, 2007. **154**(1-4): p. 103-109.
34. Hirumi, H. and K. Hirumi.Continuous cultivation of *Trypanosoma brucei* blood stream forms in a medium containing a low concentration of serum protein without feeder cell layers, *Journal of Parasitology*, 1989. **75**(6): p. 985-9.
35. Rasband, W.S., *ImageJ,* http://imagej.nih.gov/ij/. 1997-2015, U. S. National Institutes of Health, Bethesda, Maryland, USA.
36. Aslett, M., C. Aurrecoechea, M. Berriman, J. Brestelli, B.P. Brunk, M. Carrington, D.P. Depledge, S. Fischer, B. Gajria, X. Gao, *et al.*TriTrypDB: a functional genomic resource for the Trypanosomatidae, *Nucleic Acids Res*. **38**(Database issue): p. D457-62.

Type of file: figure
Label: 1
Filename: figure_1.pdf

Figure 1

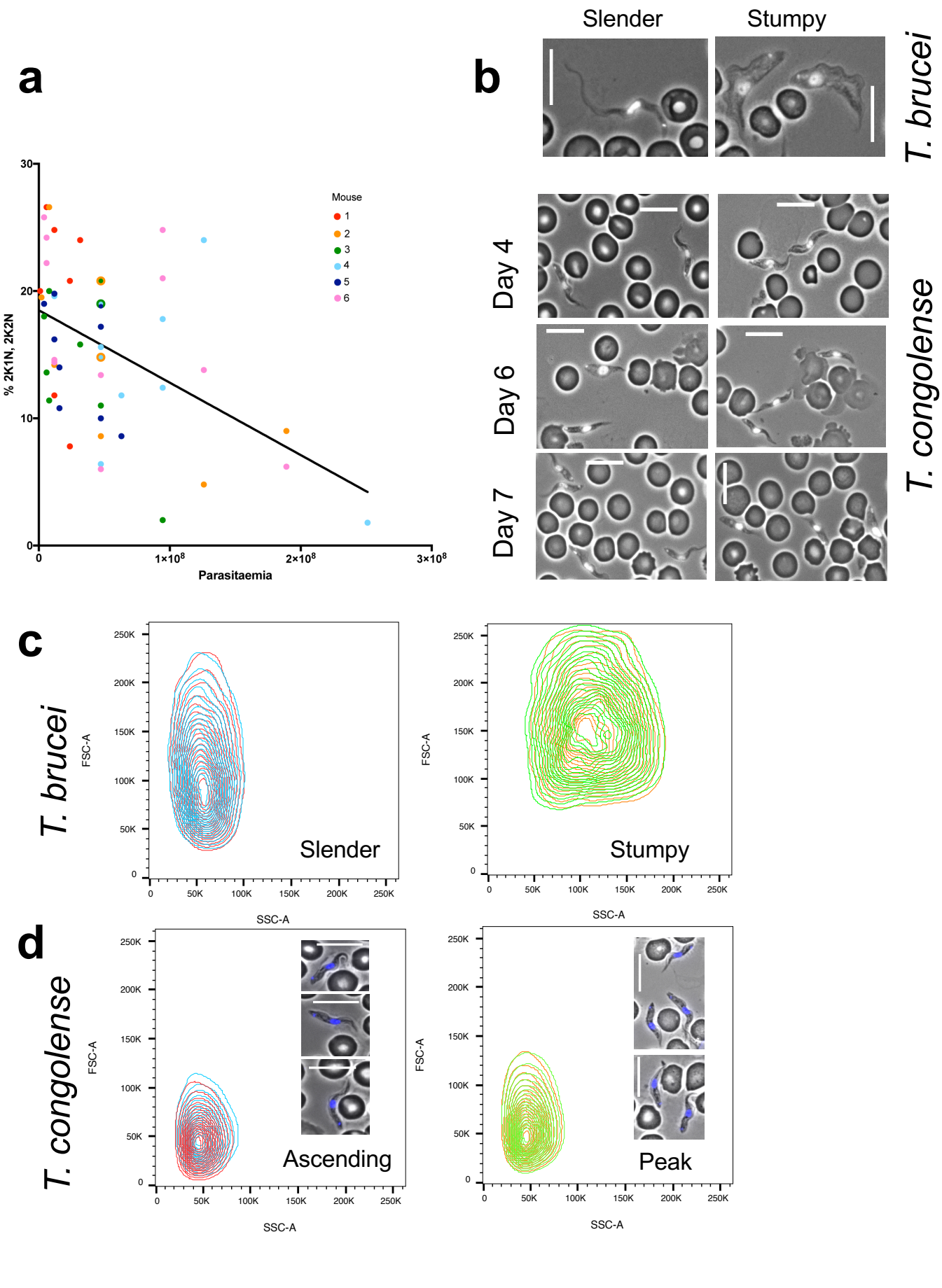
a
30
20
10
0
% 2K1N, 2K2N
Mouse
1
2
3
4
5
6
0
1×10^8
2×10^8
3×10^8
Parasitaemia
b
Slender
Stumpy
T. brucei
Day 4
Day 6
Day 7
T. congolense
c
T. brucei
FSC-A
SSC-A
250K
200K
150K
100K
50K
0
Slender
Stumpy
d
T. congolense
Ascending
Peak

Type of file: figure
Label: 2
Filename: figure_2.pdf

Figure 2

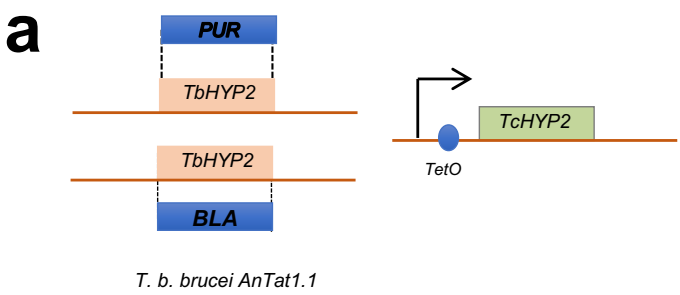
a
PUR
TbHYP2
TbHYP2
BLA
TcHYP2
TetO
T. b. brucei AnTat1.1

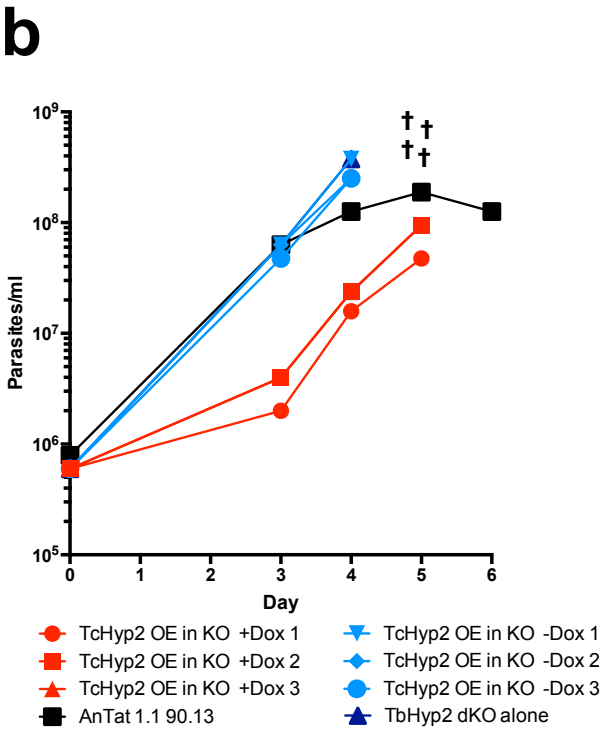
b
Parasites/ml
Day
TcHyp2 OE in KO +Dox 1
TcHyp2 OE in KO +Dox 2
TcHyp2 OE in KO +Dox 3
AnTat 1.1 90.13
TcHyp2 OE in KO -Dox 1
TcHyp2 OE in KO -Dox 2
TcHyp2 OE in KO -Dox 3
TbHyp2 dKO alone

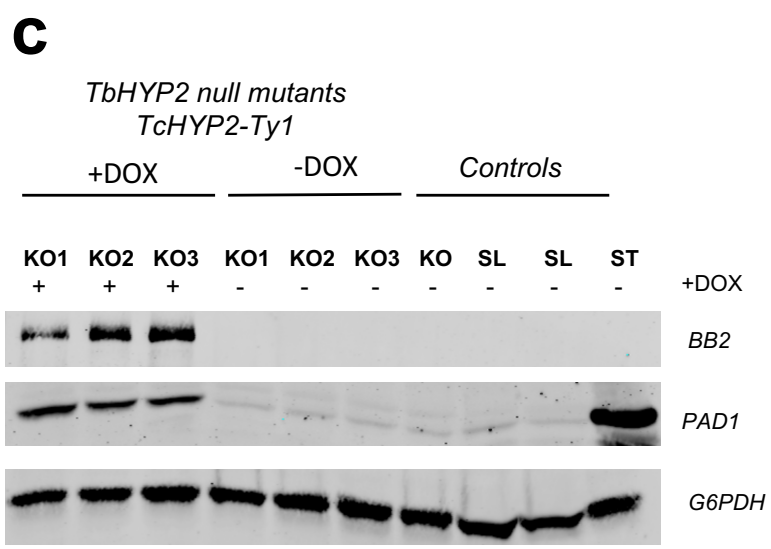
c
TbHYP2 null mutants
TcHYP2-Ty1
+DOX
-DOX
Controls
KO1 KO2 KO3 KO1 KO2 KO3 KO SL SL ST
+ + + - - - - - - -
+DOX
BB2
PAD1
G6PDH

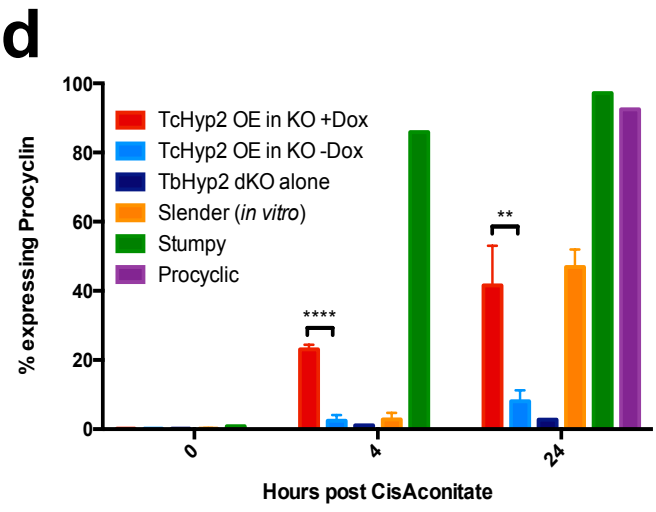
d
% expressing Procyclin
TcHyp2 OE in KO +Dox
TcHyp2 OE in KO -Dox
TbHyp2 dKO alone
Slender (in vitro)
Stumpy
Procyclic
****
**
Hours post CisAconitate

Type of file: figure
Label: 3
Filename: figure_3.pdf

Figure 3

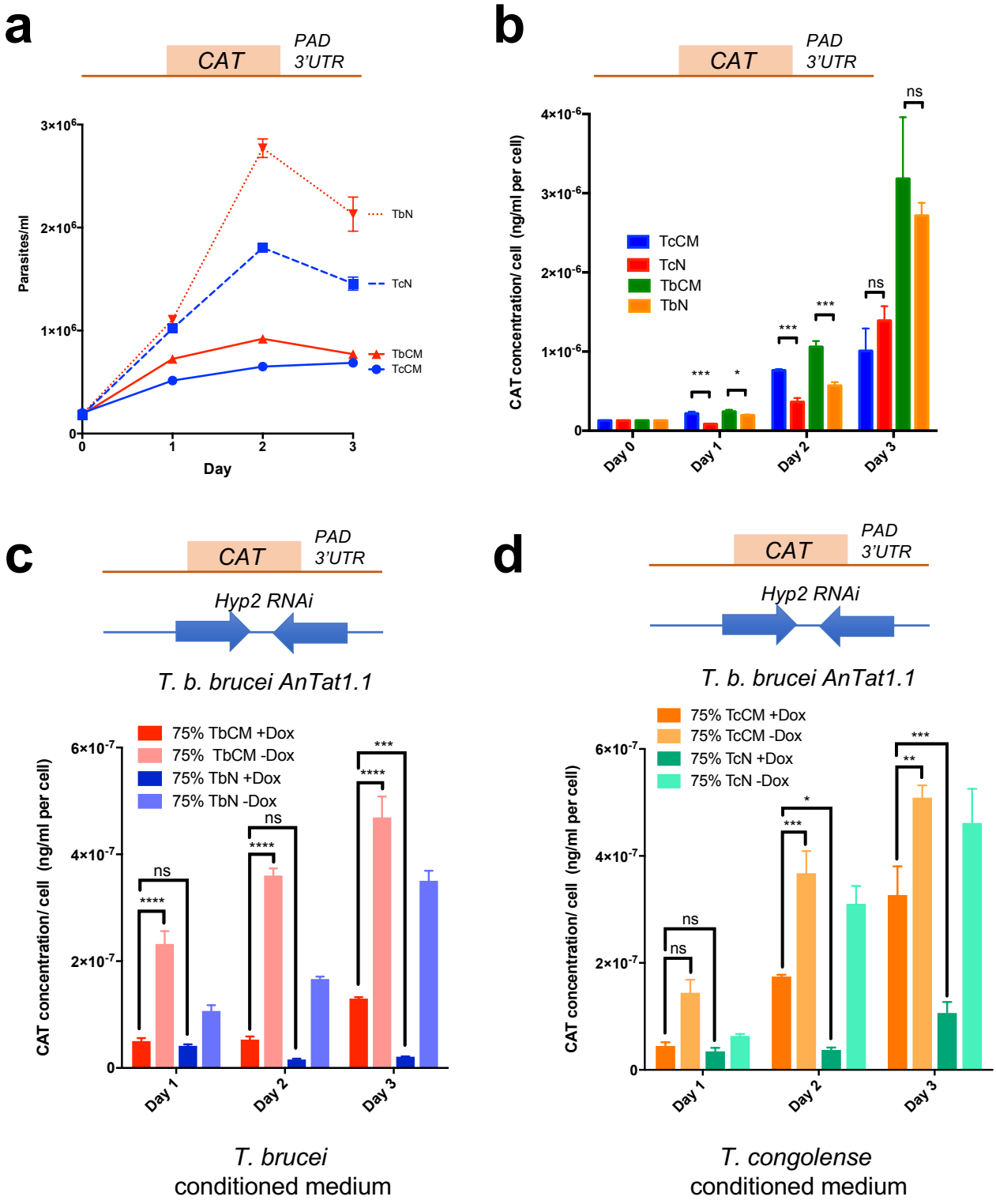
a
CAT
PAD 3'UTR
Parasites/ml
Day
TbN
TcN
TbCM
TcCM
b
CAT
PAD 3'UTR
CAT concentration/ cell (ng/ml per cell)
TcCM
TcN
TbCM
TbN
Day 0
Day 1
Day 2
Day 3
c
CAT
PAD 3'UTR
Hyp2 RNAi
T. b. brucei AnTat1.1
75% TbCM +Dox
75% TbCM -Dox
75% TbN +Dox
75% TbN -Dox
CAT concentration/ cell (ng/ml per cell)
T. brucei
conditioned medium
d
CAT
PAD 3'UTR
Hyp2 RNAi
T. b. brucei AnTat1.1
75% TcCM +Dox
75% TcCM -Dox
75% TcN +Dox
75% TcN -Dox
CAT concentration/ cell (ng/ml per cell)
T. congolense
conditioned medium

Type of file: figure
Label: 4
Filename: figure_4.pdf

Figure 4

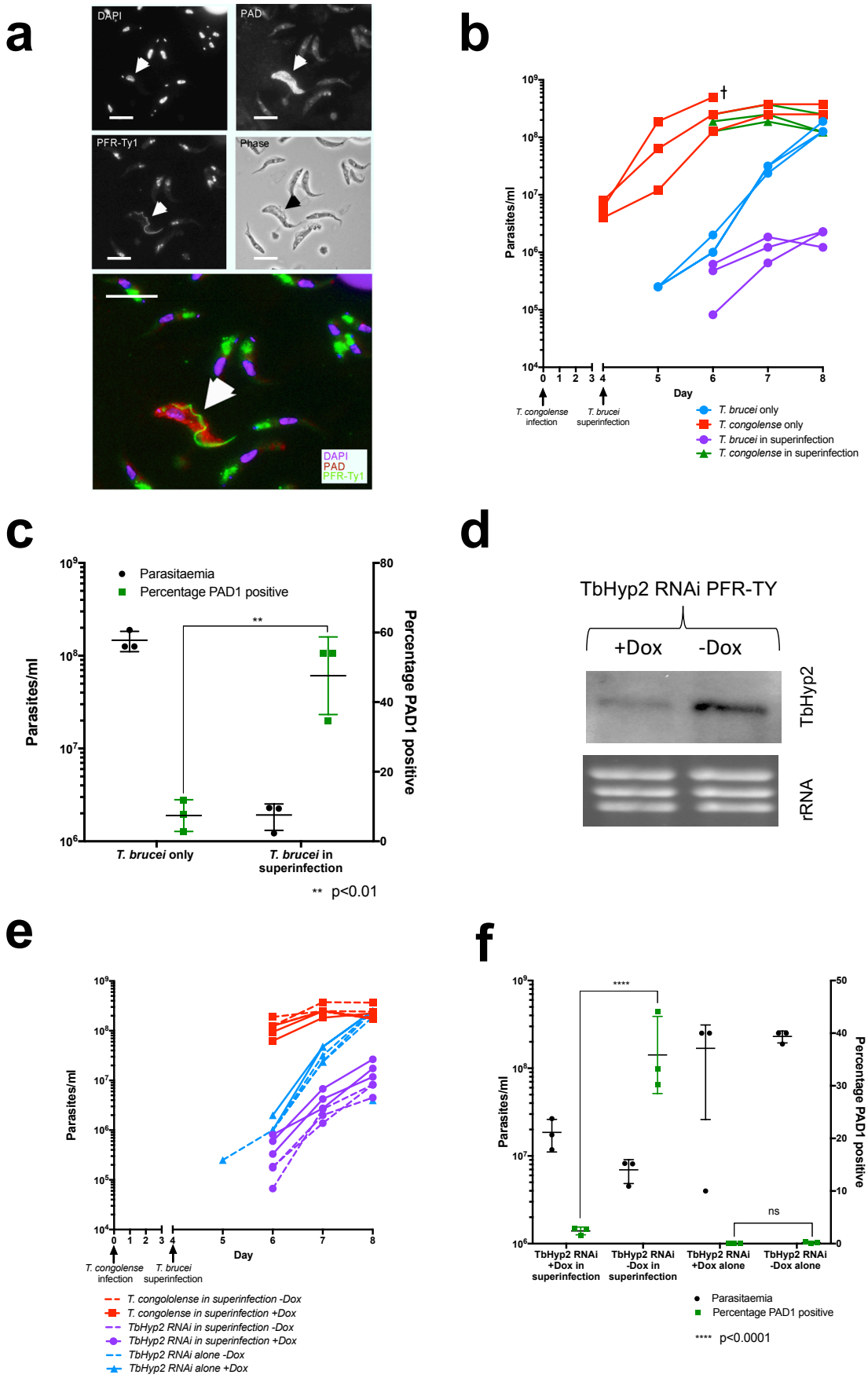
a
DAPI
PAD
PFR-Ty1
Phase
DAPI
PAD
PFR-Ty1
b
Parasites/ml
Day
T. congolense infection
T. brucei superinfection
T. brucei only
T. congolense only
T. brucei in superinfection
T. congolense in superinfection
c
Parasitaemia
Percentage PAD1 positive
Parasites/ml
Percentage PAD1 positive
T. brucei only
T. brucei in superinfection
** p<0.01
d
TbHyp2 RNAi PFR-TY
+Dox
-Dox
TbHyp2
rRNA
e
Parasites/ml
Day
T. congolense infection
T. brucei superinfection
T. congololense in superinfection -Dox
T. congolense in superinfection +Dox
TbHyp2 RNAi in superinfection -Dox
TbHyp2 RNAi in superinfection +Dox
TbHyp2 RNAi alone -Dox
TbHyp2 RNAi alone +Dox
f
Parasites/ml
Percentage PAD1 positive
****
ns
TbHyp2 RNAi +Dox in superinfection
TbHyp2 RNAi -Dox in superinfection
TbHyp2 RNAi +Dox alone
TbHyp2 RNAi -Dox alone
Parasitaemia
Percentage PAD1 positive
**** p<0.0001

Europe PMC plus has received the file 'supp_info_1.pdf' as supplementary data. The file will not appear in this PDF Receipt, but it will be linked to the web version of your manuscript.

Europe PMC plus has received the file 'supp_info_2.pdf' as supplementary data. The file will not appear in this PDF Receipt, but it will be linked to the web version of your manuscript.

Interspecies quorum-sensing in co-infections can manipulate trypanosome transmission potential

Eleanor Silvester, Julie Young, Alasdair Ivens, and Keith R. Matthews

Supplementary data

Predicted gene function	*T. brucei* ID	*T. congolense* ID	% identity	% similarity	Reciprocal BLAST?
Protein phosphatase	Tb927.4.3620	TcIL3000.11.8600	58	78	
Protein phosphatase	Tb927.4.3640	TcIL3000.11.8600	57	78	
Protein phosphatase	Tb927.4.3630	TcIL3000.11.8600	57	78	
Protein Kinase	Tb927.10.5940	TcIL3000.10.4970	89	95	●
Protein Kinase	Tb927.10.5930	TcIL3000.10.4970	90	95	
Protein Kinase	Tb927.10.5950	TcIL3000.10.4970	88	93	
Protein Kinase	Tb927.2.2720	TcIL3000.0.44450	39	54	●
Protein Kinase	Tb927.10.15020	TcIL3000.10.12870	49	63	●
Hypothetical Protein (Hyp 1)	Tb927.11.6600	TcIL3000.11.7200	46	62	●
Hypothetical Protein (Hyp 2)	Tb927.9.4080	TcIL3000.0.19510	45	58	●
RNA-binding protein	Tb927.10.12100	TcIL3000.10.10320	73	81	
Adenylosuccinate synthetase (Purine pathway)	Tb927.11.3650	TcIL3000.11.3610	86	93	●
Adenylosuccinate Lyase (Purine pathway)	Tb927.9.7550	TcIL3000.0.18960	82	91	●
GMP synthase	Tb927.7.2100	TcIL3000.0.55050	77	87	●
ubiquitin activating enzyme, putative	Tb927.2.4020	TcIL3000.2.550	54	70	●
serine/threonine protein kinase, putative	Tb927.3.4560	TcIL3000.10.4460	51	69	
hypothetical protein, conserved (Hyp 3)	Tb927.4.670	TcIL3000.4.290	59	74	●
hypothetical protein (Hyp 4)	Tb927.4.3650	TcIL3000.10.810	25	44	
adenosine kinase, putative	Tb927.6.2300	TcIL3000.6.1860	72	86	
adenosine kinase, putative	Tb927.6.2360	TcIL3000.6.1860	73	86	●
kinetoplastid-specific dual specificity phosphatase, putative	Tb927.7.7160	TcIL3000.0.52520	41	52	●
hypothetical protein, conserved (Hyp 6)	Tb927.9.13530	TcIL3000.9.5770	48	66	●
inosine-5'-monophosphate dehydrogenase	Tb927.10.16120	TcIL3000.5.1940	37	55	
phosphatase and tensin homologue, putative	Tb927.11.290	TcIL3000.11.210	67	80	●
protein kinase A regulatory subunit	Tb927.11.4610	TcIL3000.0.15340	76	88	●
transcription silencer (ISWI)	Tb927.2.1810	TcIL3000_2_50	62	76	●
Phosphoglycerate mutase	Tb927.5.3580	TcIL3000_0_40660	79	90	●
Hypothetical protein (Hyp 5)	Tb927.8.2860	TcIL3000_0_41460	40	56	●
Hypothetical protein, conserved (Hyp 8)	Tb927.11.300	TcIL3000.11.220	53	65	●
DNA repair protein, putative (Hyp 9)	Tb927.11.750	TcIL3000_0_15260	72	85	●
Product: protein phosphatase 2C, putative	Tb927.11.760	TcIL3000_0_15250	83	90	●
Hypothetical protein, conserved (Hyp 10)	Tb927.11.1640	TcIL3000.11.1420	42	60	●
Hypothetical protein, conserved (Hyp 11)	Tb927.11.2250	TcIL3000.11.2000	45	67	●
Hypothetical protein, conserved (Hyp 13)	Tb927.11.11470	TcIL3000_0_22050	66	75	●
Trichohyalin, putative	Tb927.11.11480	TcIL3000_0_28560	63	80	●

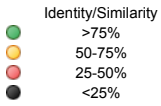

Supplementary Table 1

T. congolense encodes predicted orthologues of components of the T. brucei stumpy formation pathway.

T. brucei QS-signalling molecules were analysed by BLASTP at TritrypDB (http://tritrypdb.org/tritrypdb/). *T. congolense* was selected as the target organism and default parameters were used. The top *T. congolense* hit is reported alongside the respective % identity and % similarity of the amino acid sequences. A green dot in the final column indicates that the top *T. congolense* hit returned the original *T. brucei* protein when reciprocal BLAST was performed.

Hypothetical Protein 2 (Tb927.9.4080)	
Function or annotation	Hypothetical, conserved (HYP2)
Annotation in TritrypDB	Component of the stumpy induction factor (SIF) signalling pathway (IMP, PMID:24336212)[1] Fragments of this protein increase translation or mRNA stability when tethered to a reporter mRNA (PMID:24945722)[2] Interacts with MKT1 (PMID:24470144; IPI)[3]
RITSeq Phenotype[4]	Loss-of-fitness in differentiation from bloodstream to procyclic forms
SIF resistance[1]	RNAi targeting HYP2 results in resistance to SIF and therefore reduced stumpy formation *in vivo*
Predicted domains[5]	Prokaryotic dksA C4-type zinc finger signature and profile (InterPro IPR000962, PROSITE PS51128); P-loop containing nucleoside triphosphate hydrolases (InterPro IPR027417, Superfamily SSF52540, Gene3D G3DSA:3.40.50.300); DNA ligase/ mRNA capping enzyme (Superfamily SSF56091, Gene3D G3DSA:3.30.470.30)
Eukaryotic linear motifs[6]	Phosphorylation sites favoured by PKA-type AGC kinase (MOD_PKA_1 and _2), NEK2(MOD_NEK2_1 and _2) or CDK (MOD_CDK_1); PP1 catalytic subunit interaction motif (DOC_PP1_RVXF_1), docking motif that assists in regulating specific interactions with the MAPK cascade (DOC_MAPK_1), motif for eIF4E binding (LIG_eIF4E_1), Retinoblastoma protein interaction domain (LIG_Rb_LxCxE_1), BRCA1 interaction domain (LIG_BRCT_BRCA1_1), potential interaction with TNFR signalling pathway (LIG_TRAF2_1)
mRNA expression profile[7]	Slender – 62.6, Intermediate – 65.0, Stumpy - 59.6
Protein expression PCF/BSF[8]	1.1406
Phospho site[9]	S258

Much of this information is available in the Supplementary tables of Mony et al Nature **2014** 505 (7485): p. 681-5

Source data
1. Mony et al Nature **2014** 505 (7485): p. 681-5
2. Erben et al PLoS Pathogens **2014** 10: e1004178
3. Singh et al Nucleic acids research **2014** 42: 4652-4668
4. Alsford et al Genome Research **2011** 21: 915-924
5. Mitchell et al Nucleic acids Research **2015** 43: D213-D221
6. Dinkel et al Nucleic acids Research **2012** 40: D242-251
7. Capewell et al PLoS One **2013** 8 (6): e67069
8. Urbaniak et al PLoS One **2012** 7 (5): e36619
9. Urbaniak et al J. Proteome Res. **2013** 12 (5): pp 2233-2244

Supplementary Table 2

Characteristics of *Tb*HYP2 based on its sequence, motifs, expression and functional information available in the sources indicated.

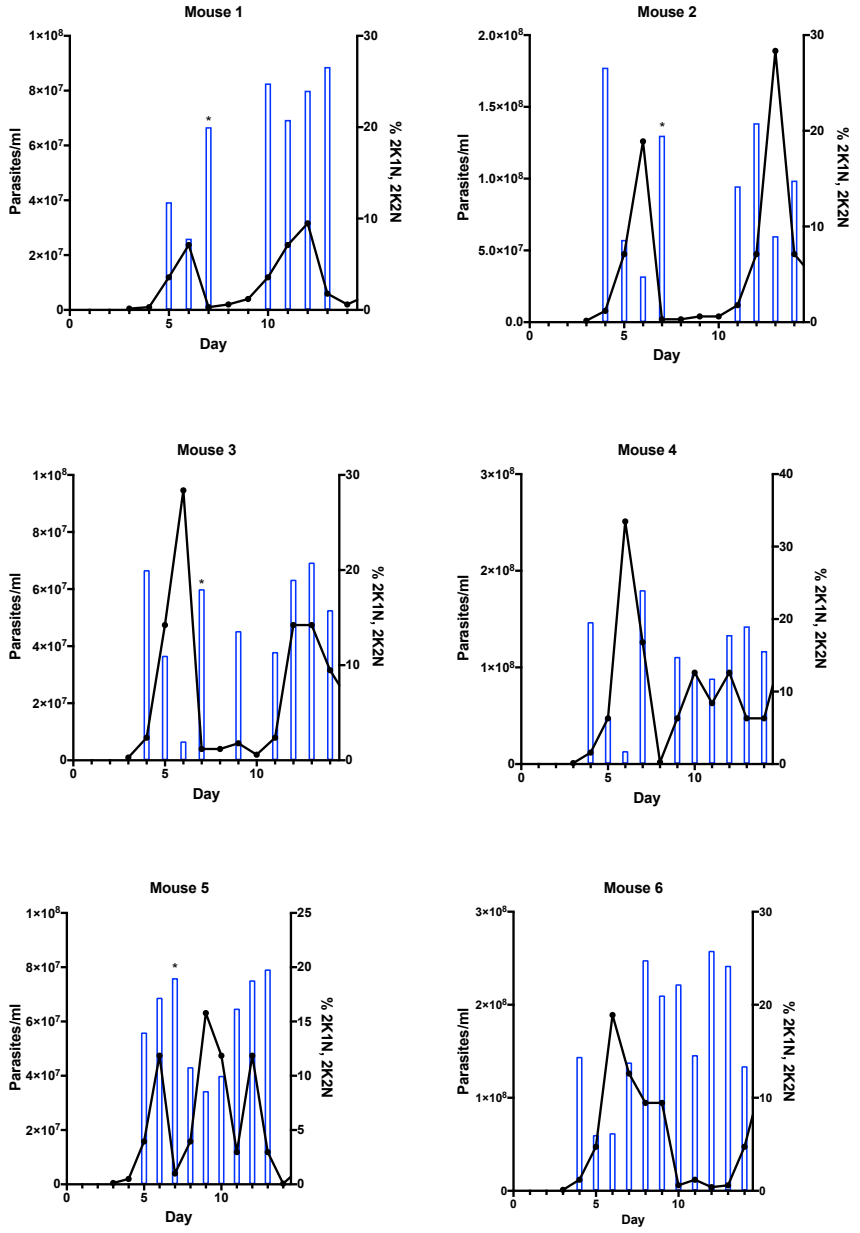

Supplementary Figure 1
Parasitaemia and cell cycle analysis for six T. congolense infections from days 3-14 post-infection.

For each infection a black line represents the parasitaemia, and blue bars represent the percentage of proliferating cells (2K1N – G2-phase cells, 2K2N – post-mitotic cells). The percentage of proliferating cells was calculated by analysing the kinetoplast and nuclear configuration of 500 cells (except for bars marked with an asterisk for which 200 cells were analysed due to the low parasitaemia at these timepoints). When parasitaemia exceeded approximately $8x10^7$/ml a reduction in proliferating cells was observed.

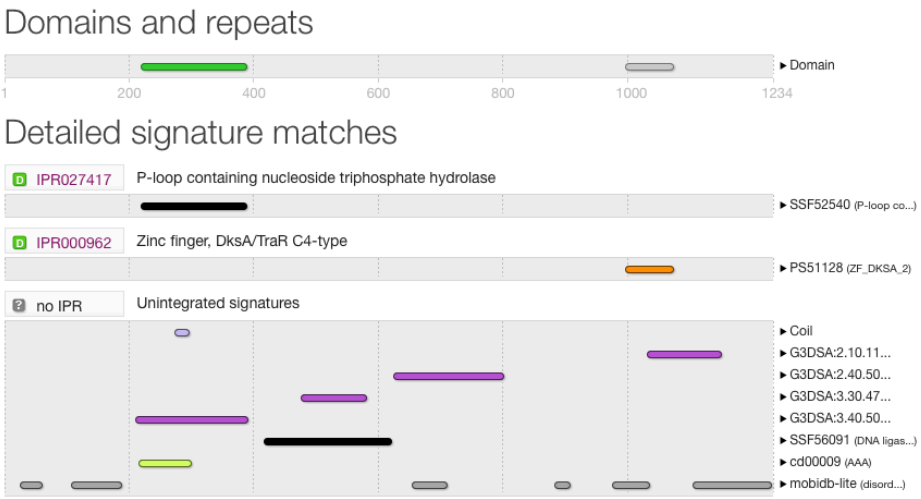

Supplementary Figure 2

Characteristics of *Tb*HYP2 showing the location of domains detected within the predicted protein

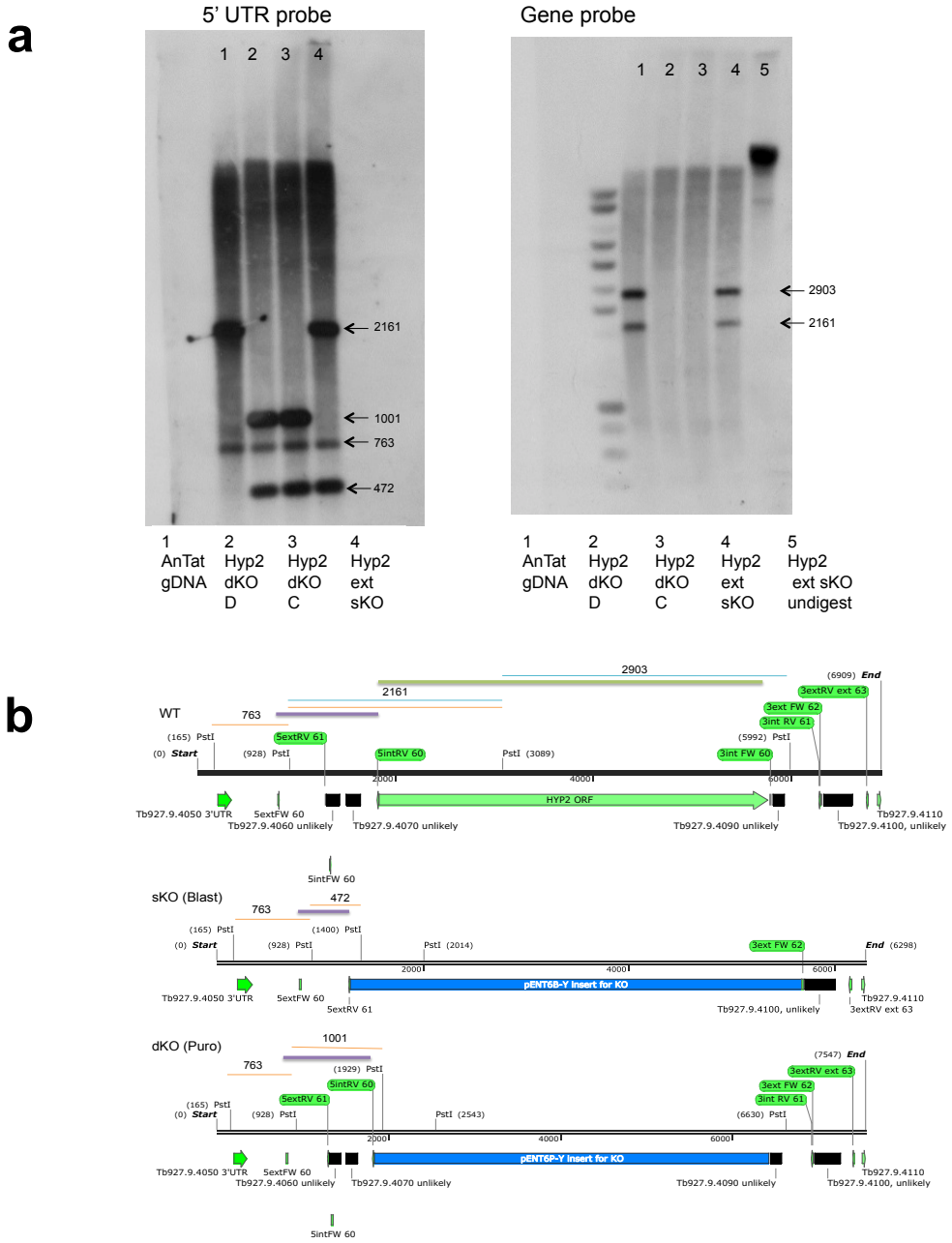

Supplementary Figure 3
*Generation of a Tb*HYP2 *(Tb927.9.4080) null mutant in a T. brucei AnTat 1.1 90.13 background.*

a) Generation of *Tb*HYP2 null mutants by sequential allelic replacement was confirmed by the restriction digest of genomic DNA from two clonal cell lines with PstI followed by Southern blotting. The use of probes targeted to either the 5'UTR or coding region of *Tb*Hyp2 revealed a characteristic digest pattern that matched expectation confirming successful generation of two *Tb*HYP2 null mutants (C and D). *Tb*HYP2 null mutant clone C was selected for further experimentation.
b) Schematic representation of expected banding patterns for the wild-type (WT) allele, the first allelic replacement (sKO) or the second allelic replacement (dKO). Predicted band sizes obtained with the 5'UTR probe are represented by orange lines, those expected with the gene probe are represented by blue lines. The total region detectable by the gene probe is represented by a thick green line. The total region detectable by the 5'UTR probe is represented by a thick purple line.

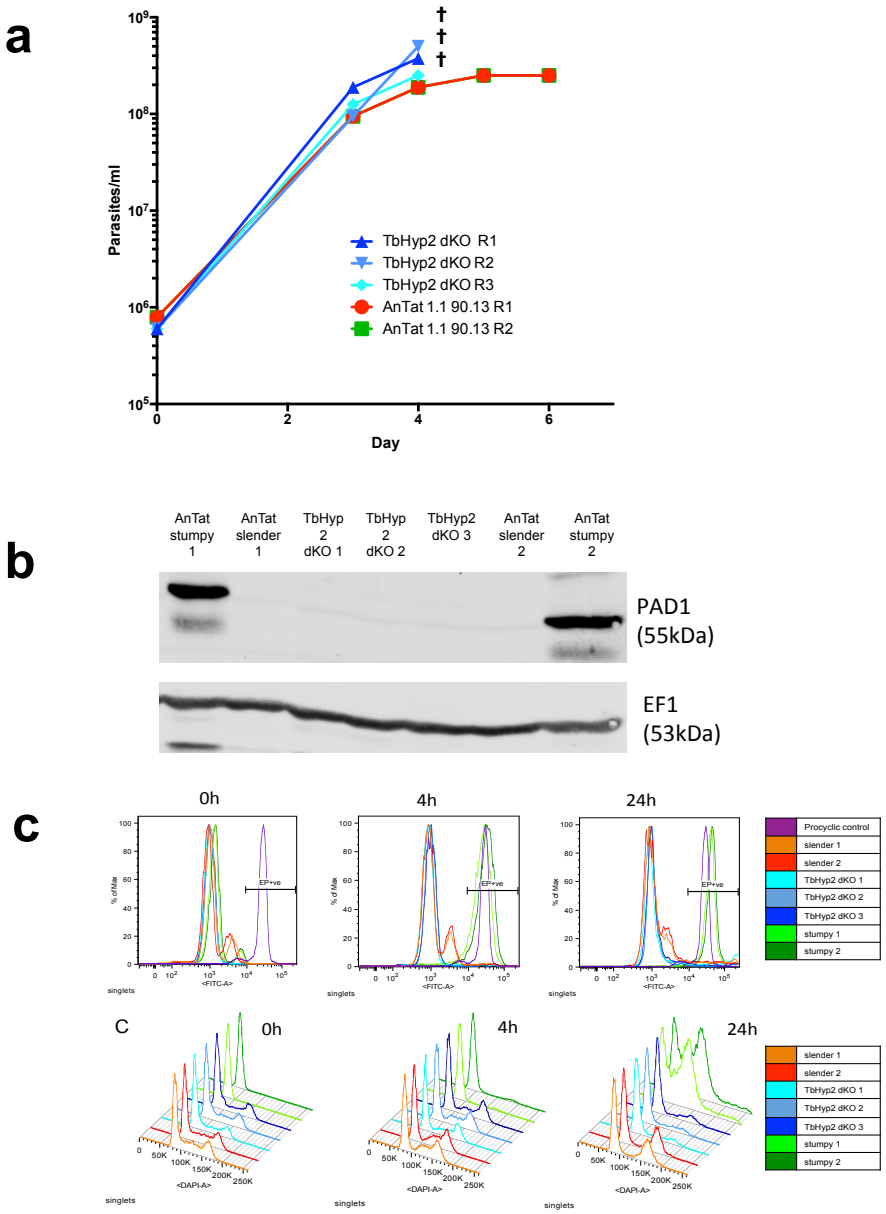

Supplementary Figure 4

*Infections with a Tb*HYP2 *null mutant reach high parasitaemia without evidence of growth control or differentiation to stumpy forms*.

a) Infections with the *Tb*HYP2 null mutant (n=3) were monitored alongside infections with the parental *T. brucei* AnTat 1.1 90.13 line (n=2). Infections were terminated when ascending parasitaemias were predicted to become lethal within 12h (crosses).

b) *Tb*HYP2 null mutant cells did not express the stumpy marker PAD1 despite high parasitaemia as visualised by western blot. EF1 was used as a loading control.

c) *Tb*HYP2 null mutant cells showed reduced capacity to differentiate to procyclic forms following induction with 6mM cis-aconitate, as determined by EP procyclin expression at 4h and 24h after induction. Additionally, *Tb*HYP2 null mutant cells showed reduced proliferation after 24h of induction with cis-aconitate, compared to both slender (3 days post infection) and stumpy (6 days post infection) control parasites. The EP procyclin expression and cell cycle data were obtained by flow cytometry.

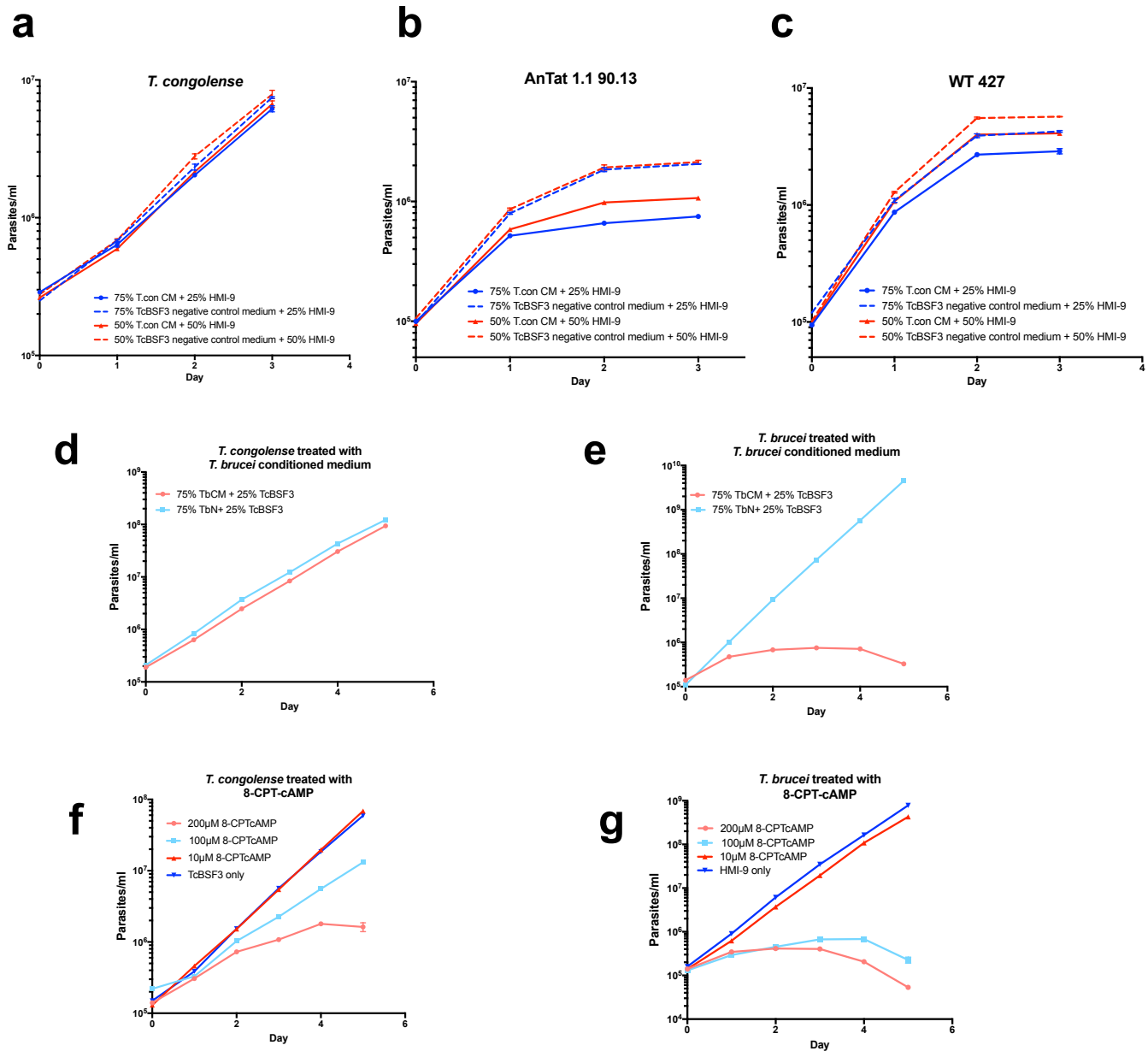

Supplementary Figure 5

a-c) The effect of T. congolense conditioned medium on T. brucei pleomorphic and monomorphic cell lines, and T. congolense itself.

d-g) The effect of T. brucei conditioned medium and 8-pCPTcAMP on T. congolense and pleomorphic T. brucei.

a) The effect of *T. congolense* conditioned medium on *T. congolense* ILTat3000.
b) The effect of *T. congolense* conditioned medium on pleomorphic *T. brucei* EATRO 1125 AnTat 1.1 90.13.
c) The effect of *T. congolense* conditioned medium on monomorphic Lister 427 *T. brucei*.
d) The effect of 75% *T. brucei* conditioned medium on *T. congolense* ILTat3000.
e) The effect of 75% *T. brucei* conditioned medium on *T. brucei* EATRO 1125 AnTat 1.1 90.13.
f) The response of *T. congolense* ILTat3000 to the cell permeable QS-signal mimic 8-pCPTcAMP.
g) The response of *T. brucei* EATRO 1125 AnTat 1.1 90.13 to the cell permeable QS-signal mimic 8-pCPTcAMP.
Each data point represents the mean of triplicate wells; errors bars represent SEM, and are sometimes obscured by the data point due to the high reproducibility of the assays.

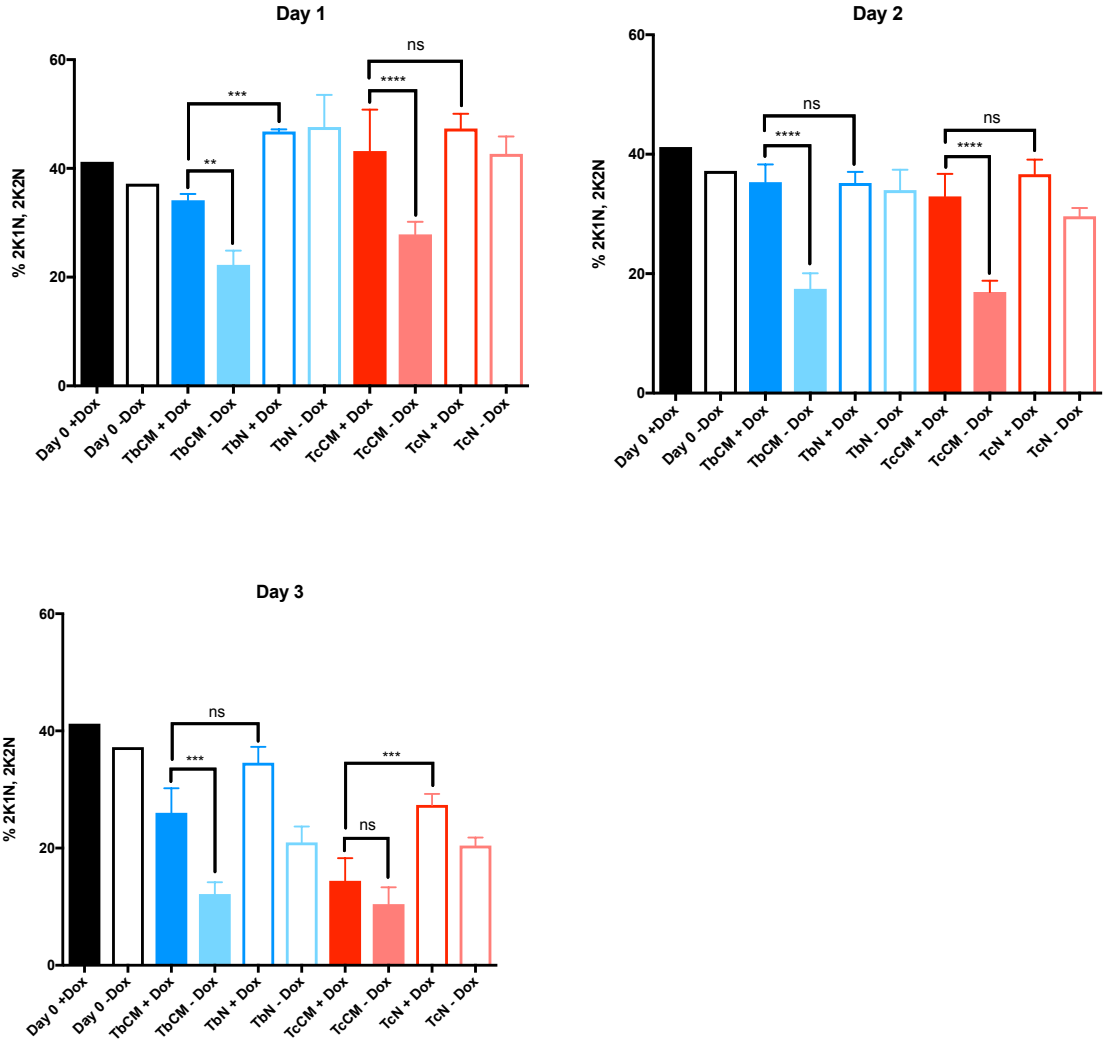

Supplementary Figure 6

Cell cycle status of T. brucei following treatment with T. brucei or T. congolense conditioned medium with (+Dox) or without (-Dox) induction of RNAi targeting TbHyp2

The pleomorphic cell line *T. brucei* AnTat 90:13 CAT-PAD *Tb*HYP2 RNAi was treated with *Tb*CM or *Tc*CM and cells collected on days 1-3 of the experiment were scored for their kinetoplast and nuclear configuration. Each bar represents the mean and standard deviation of triplicate flasks (250 cells counted for each replicate). There was a reduction in the proportion of proliferating (2K1N, 2K2N) cells following treatment with *Tb*CM or *Tc*CM when RNAi was not induced. The reduction in proliferating cells was muted when *Tb*HYP2 RNAi had been induced relative to uninduced cells. Comparisons between categories were made using two-way ANOVA followed by Tukey's multiple comparison test (★ $p<0.05$, ★★ $p<0.01$, ★★★ $p<0.001$, ★★★★ $p<0.0001$). The effect of *Tc*CM and *Tb*CM on this cell line was reproducible in two independent experiments (one representative experiment is shown).

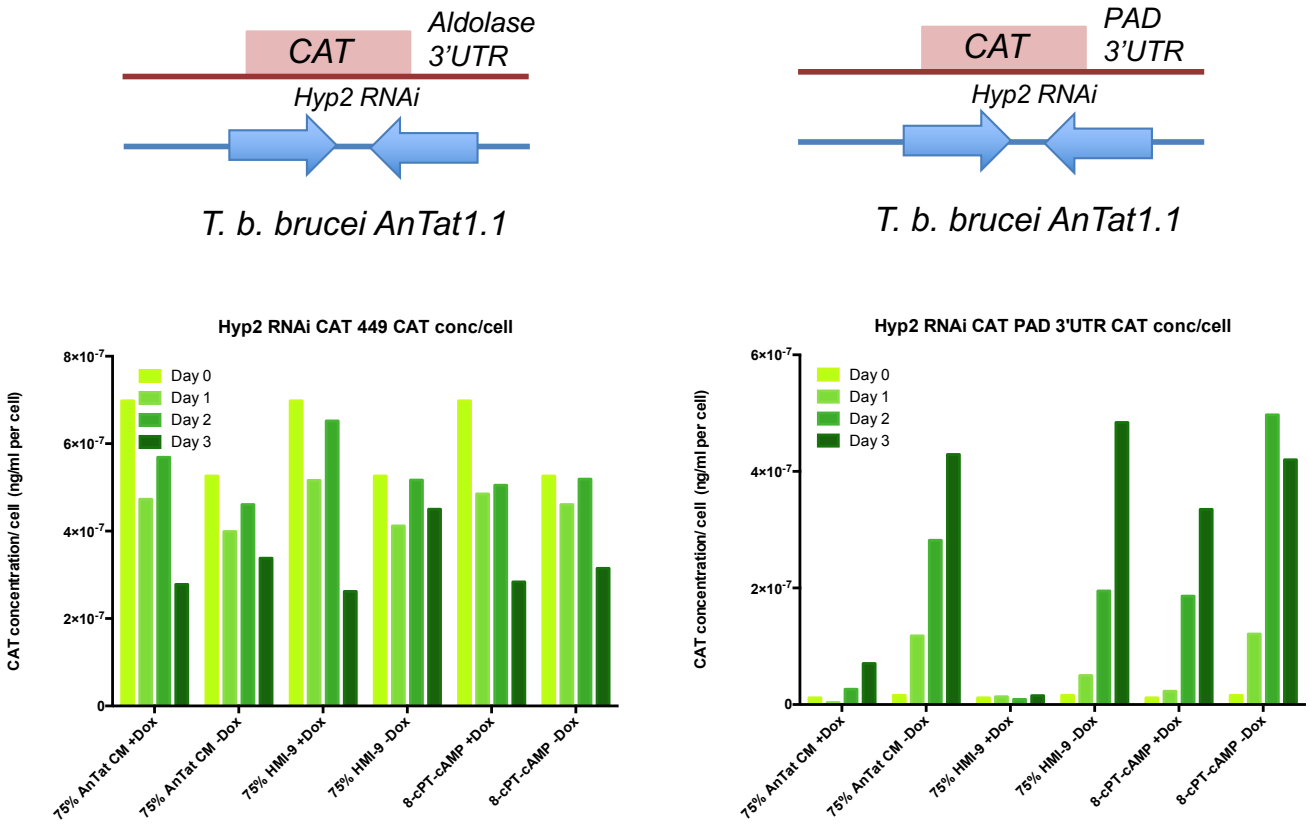

Supplementary Figure 7

*The effect of T. brucei conditioned medium and 8-pCPT-cAMP on a pleomorphic reporter line with inducible Tb*HYP2 *RNAi.*

A pleomorphic *T. brucei* cell line (EATRO 1125; AnTat 1.1 90.13) capable of doxycycline inducible knock down of *Tb*HYP2 was transfected with either of two constructs. One construct encoded a CAT reporter with expression under the control of an aldolase 3'UTR. When the cell line with this control construct was treated with conditioned medium or the QS-signal mimic 8-pCPT-cAMP there was no effect on CAT concentration/cell related to RNAi against *Tb*HYP2. The second construct encoded a CAT reporter with expression under the control of the PAD1 3'UTR. When the cell line with the CAT PAD construct was treated with conditioned medium (AnTat CM) or 8-pCPT-cAMP the CAT concentration/cell increased relative to the negative control (75% HMI-9). However, when *Tb*HYP2 RNAi was induced (+Dox) the CAT concentration/cell did not increase with conditioned medium treatment. For each condition tested n=1.

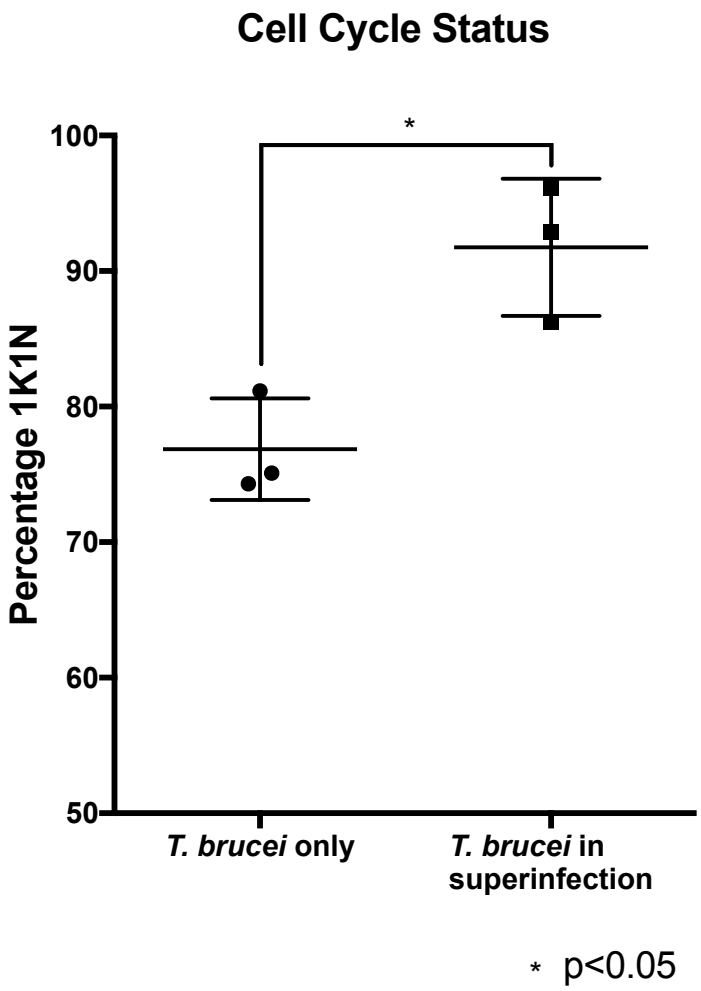

Supplementary Figure 8
Cell cycle status of T. brucei in co-infection with T. congolense or in a single species infection.

T. brucei cells collected on day 8 of the experiment were scored for their kinetoplast and nuclear configuration (>500 cells scored, n=3 for each condition tested). Error bars represent mean ± SD. The lower *T. brucei* parasitaemia in the superinfections was associated with a significantly higher proportion of 1K1N cells compared to that observed in the single species *T. brucei* infections (unpaired t test, ★ $p<0.05$, two-sided).

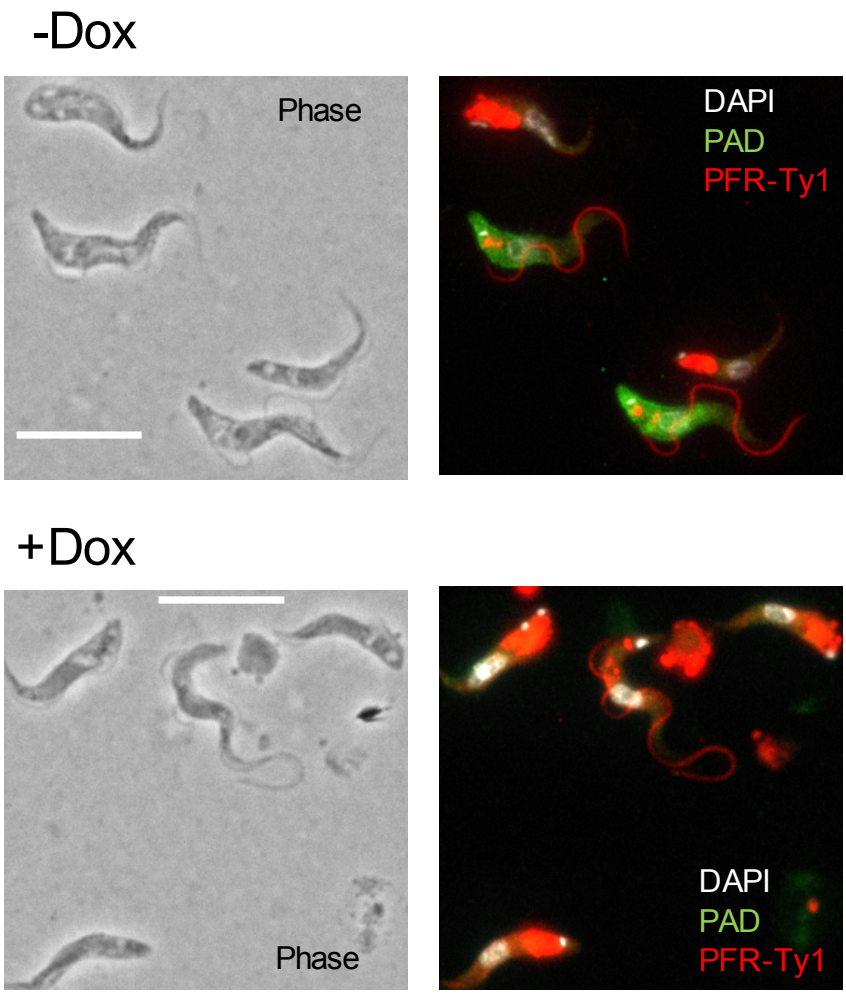

Supplementary Figure 9
Representative images of day 8 superinfection samples with (+Dox) or without (-Dox) induction of RNAi targeting TbHyp2.

An example of PAD1-positive intermediate/stumpy *T. brucei* cells accompanied by *T. congolense* on day 8 of the co-infection experiment when *Tb*Hyp2 RNAi has not been induced (-Dox), and an example of a PAD1-negative, slender, *T. brucei* cell accompanied by *T. congolense* when *Tb*HYP2 RNAi has been induced (+Dox). PFR-Ty1 (red), PAD1 (green), DAPI (white). Note that *T. congolense* cells show non-specific intracellular staining with the BB2 antibody that detects the Ty1 epitope. Scale bar represents 10μm

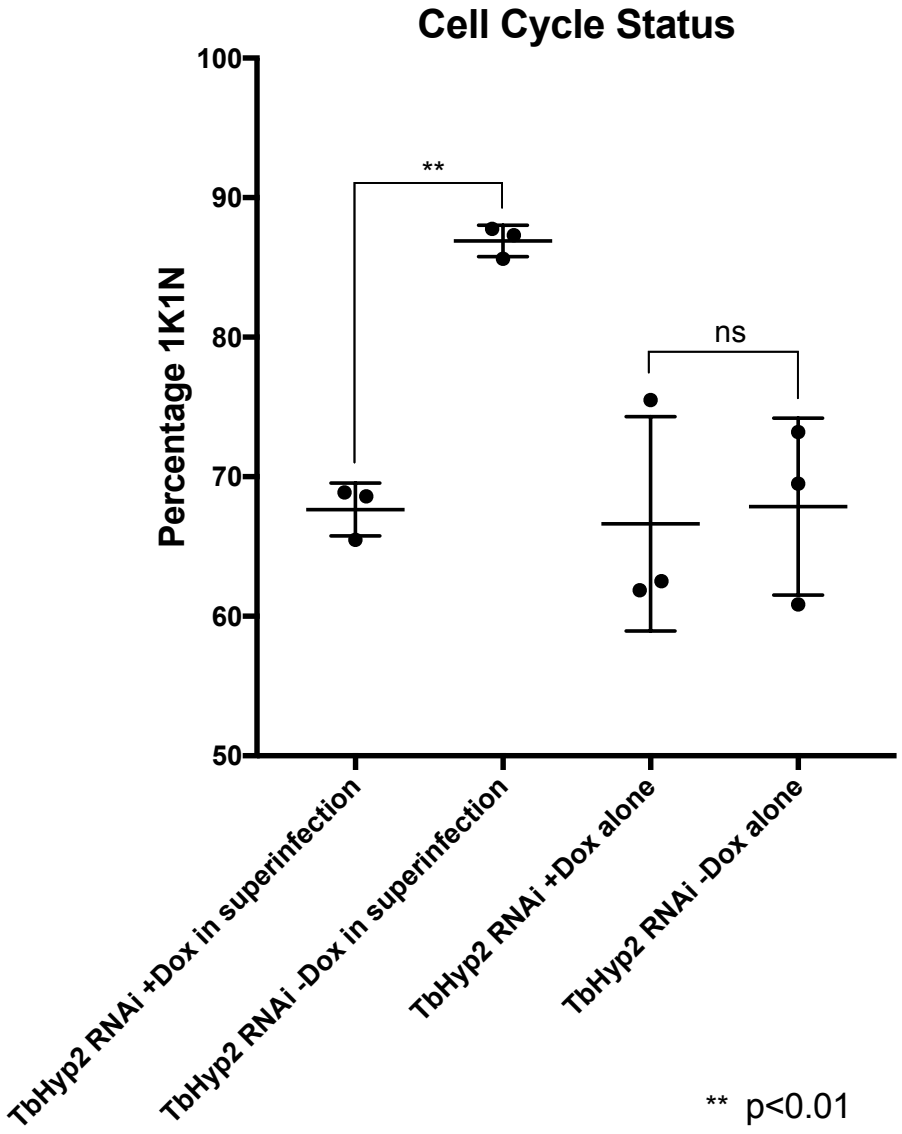

Supplementary Figure 10
*Cell cycle status of T. brucei in co-infection with T. congolense or in a single species infection with or without the induction of RNAi targeting Tb*HYP2.

T. brucei cells collected on day 8 of the experiment were scored for their kinetoplast and nuclear configuration (>500 cells scored, n=3 for each condition tested). Error bars represent mean ± SD. There was a significantly higher proportion of 1K1N *T. brucei* cells when *Tb*HYP2 RNAi was not induced (-Dox), than when *Tb*HYP2 RNAi was induced (+Dox) in a co-infection with *T. congolense* (★★ p<0.01, One-way ANOVA with Tukey's multiple comparisons test).

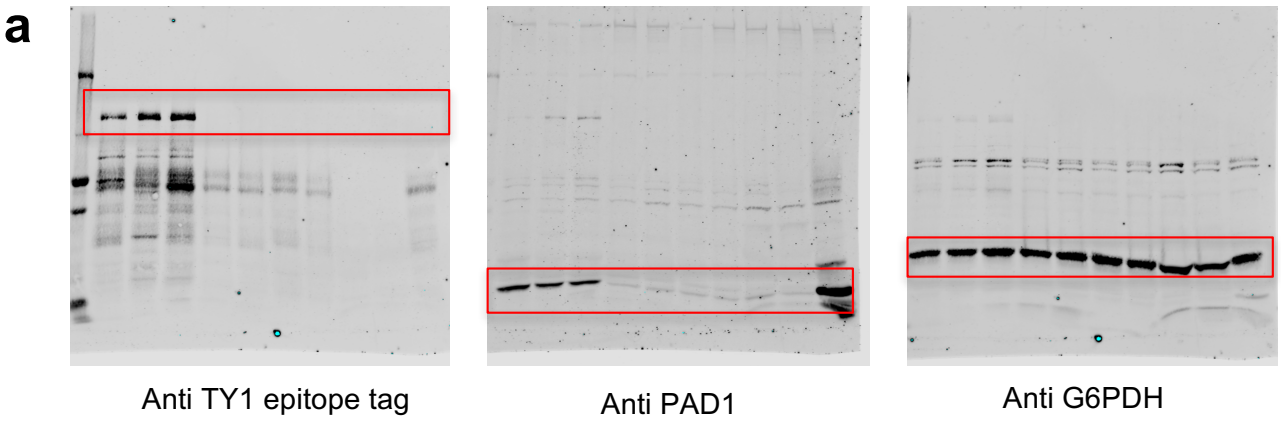

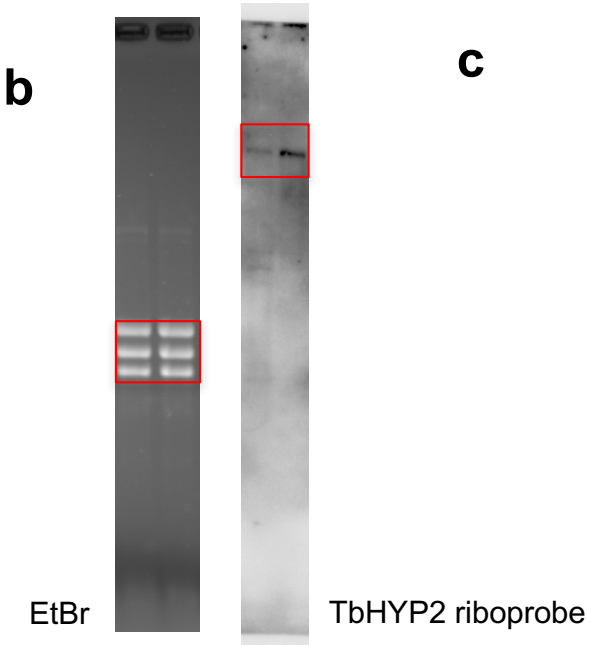

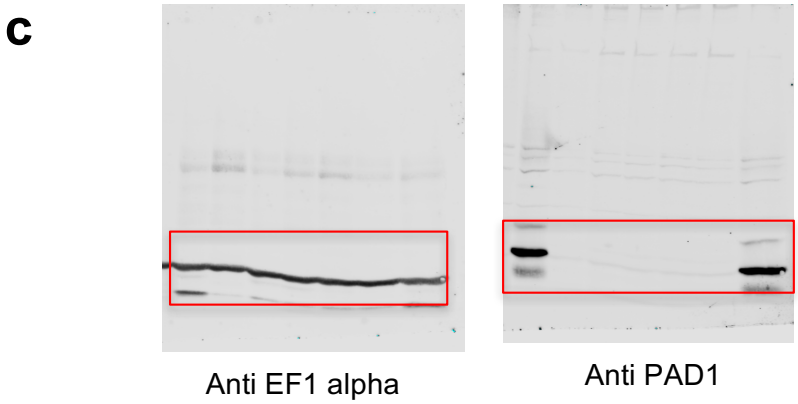

Supplementary Figure 11.

Full length gels and blots from the Figures presented in this paper.

a. Figure 2c blots
b. Figure 4 d blots
c. Supplementary Figure 4b blots